



**CHALMERS**  
UNIVERSITY OF TECHNOLOGY



# **Islanded Operation of Wind Turbine with Solar Power and Battery Storage**

**A Power-Balance-Oriented Energy Management Approach**

Master's thesis in Sustainable Electric Power Engineering and Electromobility

**TIANXING XU, YICHI ZHANG**

**DEPARTMENT OF ELECTRICAL ENGINEERING**

**CHALMERS UNIVERSITY OF TECHNOLOGY**

Gothenburg, Sweden 2026

[www.chalmers.se](http://www.chalmers.se)



MASTER'S THESIS 2026

# Islanded Operation of Wind Turbine with Solar Power and Battery Storage

A Power-Balance-Oriented Energy Management Approach

TIANXING XU, YICHI ZHANG



**CHALMERS**  
UNIVERSITY OF TECHNOLOGY

Department of Electrical Engineering  
*Division of Electric Power Engineering*  
CHALMERS UNIVERSITY OF TECHNOLOGY  
Gothenburg, Sweden 2026

Islanded Operation of Wind Turbine with Solar Power and Battery Storage  
A Power-Balance-Oriented Energy Management Approach  
TIANXING XU, YICHI ZHANG

© TIANXING XU, YICHI ZHANG, 2026.

Supervisor: Prof. Ola Carlson, Department of Electrical Engineering  
Examiner: Prof. Ola Carlson, Department of Electrical Engineering

Master's Thesis 2026  
Department of Electrical Engineering  
Division of Electric Power Engineering  
Chalmers University of Technology  
SE-412 96 Gothenburg  
Telephone +46 31 772 1000

Cover: Wind turbine related illustration from the Chalmers thesis template.

Typeset in L<sup>A</sup>T<sub>E</sub>X  
Printed by Chalmers Reproservice  
Gothenburg, Sweden 2026

Islanded Operation of Wind Turbine with Solar Power and Battery Storage  
A Power-Balance-Oriented Energy Management Approach  
Tianxing Xu, Yichi Zhang  
Department of Electrical Engineering  
Chalmers University of Technology

## Abstract

This thesis studies the monitoring and control of an islanded hybrid power system composed of a wind turbine, photovoltaic generation, a battery energy storage system, and local load demand. The motivation of the study is that when the system operates without the continuous support of the external power grid, it needs to coordinate local power generation and energy storage. Therefore, the research focuses on the analysis of active power balance, battery dispatch, wind-power curtailment, load shedding and wind turbine response under islanded operating conditions.

A layered modelling strategy is used in MATLAB/Simulink. The inherited wind-turbine model is kept as the wind-side technical basis, and the main work of this thesis is to build and connect an Energy Management System (EMS) around it. The EMS takes the realised wind-turbine output, an equivalent AC-side photovoltaic active-power contribution, load demand, and battery state of charge as inputs. It then calculates the battery-power reference, the constrained battery response, the residual mismatch quantities, the wind-curtailment request, and the load-shedding request. In this work, the available wind-power estimate and the realised simulated wind-turbine output are not treated as the same signal. The available wind-power signal is used as a wind-side availability reference, while the realised wind-turbine output is the simulated power after the turbine dynamics and, when it is active, the wind-spill and blade-pitch action.

An important implementation point is that the EMS curtailment request is sent to the inherited wind-spill input as a spilling-power command. Therefore, curtailment is represented through the turbine-side control path, rather than by directly subtracting power from the wind-power signal. In the short-term integrated simulation, the EMS response is analysed together with the simulated blade-pitch response, the wind-spill command, and the realised wind-turbine power. The results show a change from an initial deficit condition to a surplus condition. After this change, the battery charging becomes constrained, residual surplus is formed, the wind-spill request is activated, and the realised simulated wind-turbine output is reduced.

A complementary long-term EMS/BESS simulation is performed over an 1800 s horizon using prescribed wind, PV, and load input profiles. The battery-power reference, constrained battery power, SOC evolution, original and residual mismatch quantities, and corrective-action requests are analysed as simulation outputs of the developed supervisory controller. The long-term results show that the battery first absorbs renewable surplus within its implemented charging and SOC constraints, while remaining residual surplus is assigned to wind-power curtailment.

An additional deficit-dominated EMS-level case is included to verify the load-shedding branch of the supervisory controller. In this case, an imposed high-load interval produces a power deficit that exceeds the allowable battery discharge response. The

---

battery first supplies power within its implemented limit, after which the remaining residual deficit is converted into a load-shedding request. This case complements the surplus-dominated long-term case and confirms the intended priority order of the EMS under both surplus and deficit conditions.

This thesis shows that the developed supervisory structure provides a useful simulation framework for the operation of an islanded wind-solar-battery system. The study clarifies the difference between prescribed operating inputs, inherited wind-model quantities, and simulated EMS/BESS outputs; it also gives a basis for future work on more detailed converter-level implementation, improved battery modelling, and wider islanded microgrid studies.

Keywords: islanded operation, wind turbine, photovoltaic generation, battery energy storage, energy management system, wind curtailment, load shedding, Simulink, microgrid.



# Acknowledgements

We would like to express our sincere gratitude to Professor Ola Carlson for his supervision, guidance, and valuable feedback throughout this thesis work. His comments helped us clarify the scope of the project and focus the work on a supervisory control formulation that is technically meaningful and feasible within the time frame of a master's thesis.

We are also grateful to Victor Kattokola for his careful proofreading and constructive comments on the thesis manuscript.

Our thanks are extended to the Department of Electrical Engineering and the Division of Electric Power Engineering at Chalmers University of Technology for providing the academic environment, technical background, and modelling resources that supported this project.

We would also like to acknowledge the authors of previous thesis work on the Chalmers wind turbine and islanded-operation studies. Their work provided an important foundation for understanding the inherited wind-turbine model and the broader context of wind-power-based islanded operation.

Finally, we appreciate the support received from discussions, coursework, and the broader research environment at Chalmers during the modelling and writing process.

Tianxing Xu, Yichi Zhang, Gothenburg, May 2026





# List of Acronyms

Below is the list of acronyms that have been used throughout this thesis listed in alphabetical order:

BESS	Battery Energy Storage System
DER	Distributed Energy Resource
EMS	Energy Management System
FFR	Fast Frequency Reserve
FCR	Frequency Containment Reserve
GFM	Grid-Forming
MG	Microgrid
MPPT	Maximum Power Point Tracking
PV	Photovoltaic
RES	Renewable Energy Sources
RMS	Root Mean Square
SOC	State of Charge
SPS	Specialized Power Systems
TSR	Tip Speed Ratio



# Nomenclature

Below is the nomenclature of selected parameters and variables used throughout this thesis. The notation distinguishes between available wind power, realised simulated wind-turbine output, EMS-generated supervisory variables, and measurement-derived or replay input signals.

## Parameters

$A$	Rotor swept area
$C_p$	Power coefficient of the wind turbine
$E_{\text{nom}}$	Nominal stored energy of the battery
$P_{\text{ch,max}}$	Maximum battery charging-power magnitude; charging appears as negative battery power
$P_{\text{dis,max}}$	Maximum battery discharging-power magnitude
$Q_{\text{nom}}$	Nominal battery charge capacity
$R$	Rotor radius
$SOC_{\text{max}}$	Upper state-of-charge threshold applied in the supervisory battery logic
$SOC_{\text{min}}$	Lower state-of-charge threshold applied in the supervisory battery logic
$V_{\text{nom}}$	Nominal battery voltage
$\rho$	Air density
$\lambda$	Tip-speed ratio

## Variables

$\beta$	Blade-pitch angle
$\beta_{\text{sim}}$	Simulated blade-pitch response generated by the inherited wind-turbine model
$\omega_r$	Rotor angular speed

---

$\omega_{\text{turb}}$	Turbine rotational speed
$v$	Wind speed
$v_{\text{est}}$	Estimated wind-speed signal generated inside the inherited wind-turbine model
$v_{\text{meas}}$	Measured wind-speed input signal
$I_{\text{batt}}$	Battery current used for SOC calculation in the simplified BESS interface
$I_{\text{cmd}}$	Current command derived from the EMS battery-power command
$P_{\text{batt}}$	Final constrained battery power generated by the EMS/BESS interface; positive values denote discharge and negative values denote charge
$P_{\text{batt,cha}}$	Battery charging-branch output before recombination into $P_{\text{batt}}$
$P_{\text{batt,dis}}$	Battery discharging-branch output before recombination into $P_{\text{batt}}$
$P_{\text{batt,eff}}$	Effective battery power used in downstream supervisory power-balance interpretation
$P_{\text{batt,ref}}$	Battery-reference power before battery-power and SOC limitations
$P_{\text{curt}}$	EMS wind-curtailment request generated from residual surplus
$P_{\text{deficit}}$	Original power deficit before battery action
$P_{\text{deficit,res}}$	Residual power deficit after battery action
$P_{\text{err}}$	Remaining mismatch after feasible battery action
$P_{\text{gen}}$	Generic generation contribution in the general islanded-system balance; represented by $P_{\text{ren}}$ within the implemented system
$P_{\text{load}}$	Original load demand
$P_{\text{load,eff}}$	Effective load after load-shedding correction
$P_{\text{loadshed}}$	Load-shedding request generated from residual deficit
$P_{\text{loss}}$	Aggregated electrical and conversion loss term used only in the general system-level balance background; not implemented as a separate EMS input signal
$P_{\text{net}}$	Net active-power quantity used for downstream supervisory power-balance interpretation
$P_{\text{pv}}$	Equivalent AC-side photovoltaic active-power contribution supplied to the EMS power-balance interface
$P_{\text{pv,avail}}$	Equivalent photovoltaic active power available at the EMS interface after an unmodelled PV conversion stage
$P_{\text{pv,eff}}$	Effective photovoltaic power used in downstream supervisory power-balance interpretation

---

$P_{\text{ren}}$	Aggregated renewable power used in the implemented EMS; $P_{\text{ren}} = P_{\text{wind}} + P_{\text{pv}}$ and represents the generation contribution within the implemented model
$P_{\text{spill}}$	Spilling-power command passed to the inherited wind-spill path; $P_{\text{spill}} = P_{\text{curt}}$ in the implemented connection
$P_{\text{storage}}$	Generic storage contribution in the islanded-system power-balance background
$P_{\text{surplus}}$	Original power surplus before battery action
$P_{\text{surplus,res}}$	Residual power surplus after battery action
$P_{\text{wind}}$	Realised simulated wind-turbine output after inherited turbine dynamics and, when activated, the wind-spill and blade-pitch response; used in the EMS and Wind Curtailment subsystem
$P_{\text{wind,avail}}$	Rated-power-capped available wind-power estimate generated by the inherited wind-turbine model; retained as a wind-side availability reference
$P_{\text{wind,down}}$	Wind contribution used in downstream supervisory power-balance interpretation; $P_{\text{wind,down}} = P_{\text{wind}}$
$P_{\text{wind,mech}}$	Aerodynamic mechanical wind power in the wind-turbine theory background
$SOC$	Battery state of charge
$\Delta P$	Conceptual active-power mismatch in the general islanded-system background



# Contents

<b>List of Acronyms</b>	<b>x</b>
<b>Nomenclature</b>	<b>xiii</b>
<b>List of Figures</b>	<b>xxi</b>
<b>List of Tables</b>	<b>xxiii</b>
<b>1 Introduction</b>	<b>1</b>
1.1 Background . . . . .	1
1.2 Literature Review and Research Gap . . . . .	2
1.2.1 Microgrid Control Architecture . . . . .	2
1.2.2 EMS Design for Hybrid Renewable Systems . . . . .	3
1.2.3 Simplified Models for Islanded-Control Evaluation . . . . .	4
1.2.4 Previous Chalmers Work and the Inherited Wind-Turbine Model . . . . .	4
1.2.5 Research Gap Addressed in This Thesis . . . . .	5
1.3 Aim and Scope . . . . .	5
1.4 Research Questions . . . . .	6
1.5 Scientific and Engineering Contribution . . . . .	6
1.6 Methodological Overview . . . . .	7
1.7 Thesis Structure . . . . .	7
<b>2 Theory and Modelling Background</b>	<b>9</b>
2.1 Islanded Hybrid Power Systems . . . . .	9
2.2 Operational Challenges in Islanded Mode . . . . .	10
2.3 Supervisory Control Scope and Modelling Boundary . . . . .	11
2.4 Wind-Turbine Power Background . . . . .	11
2.5 Photovoltaic Power Representation . . . . .	12
2.6 Battery Energy Storage in Islanded Operation . . . . .	13
2.7 Energy Management System as a Supervisory Layer . . . . .	13
2.8 Supervisory Power-Balance Formulation . . . . .	14
2.9 Battery Constraint Logic . . . . .	14
2.10 Residual Mismatch and Corrective Actions . . . . .	15
2.11 Wind Curtailment and Load Shedding . . . . .	15
2.11.1 Wind Curtailment . . . . .	15
2.11.2 Load Shedding . . . . .	16
2.12 Corrected Power Variables and Interface Logic . . . . .	16

2.13	Hierarchical Modelling Philosophy . . . . .	17
2.14	Modelling Scope of the Theory . . . . .	17
<b>3</b>	<b>Methods and Implementation</b>	<b>19</b>
3.1	Overall Modelling Strategy . . . . .	19
3.2	Simulation Environment and Modelling Boundary . . . . .	20
3.3	Inherited Wind-Turbine Subsystem . . . . .	20
3.4	EMS–BESS–Interface Architecture . . . . .	21
3.5	Supervisory Control Sequence . . . . .	21
3.6	Implemented EMS Signal Structure . . . . .	23
3.7	Battery Dispatch and BESS Interface . . . . .	24
3.8	Residual Mismatch and Corrective-Action Paths . . . . .	26
3.9	Implemented Wind-Curtailment Connection . . . . .	26
3.10	Implemented Load-Shedding Path . . . . .	27
3.11	System-Level Interface and Monitored Variables . . . . .	27
3.12	Long-Term EMS/BESS Simulation . . . . .	29
3.13	Short-Term Integrated EMS–Wind-Turbine Simulation . . . . .	30
3.14	Traceability from Theory to Implementation . . . . .	30
3.15	Implementation Scope . . . . .	31
<b>4</b>	<b>Results and Discussion</b>	<b>33</b>
4.1	Overview of the Result Analysis . . . . .	33
4.2	Classification of Result Signals . . . . .	34
4.3	Simulation Parameters Used in the Result Cases . . . . .	34
4.4	Long-Term EMS/BESS Simulation . . . . .	36
4.4.1	Long-Term Source and Load Profiles . . . . .	36
4.4.2	Battery Reference and Constrained Battery Power . . . . .	37
4.4.3	Original Deficit and Surplus . . . . .	37
4.4.4	Simulated SOC Evolution . . . . .	37
4.4.5	Residual Mismatch After Battery Action . . . . .	39
4.4.6	Curtailment and Load-Shedding Requests . . . . .	39
4.5	Additional Deficit and Load-Shedding Validation Case . . . . .	40
4.5.1	Purpose of the Additional Validation Case . . . . .	40
4.5.2	Prescribed Load Profile . . . . .	40
4.5.3	Original Power Deficit . . . . .	41
4.5.4	Battery Response in the Deficit Case . . . . .	42
4.5.5	Simulated SOC in the Deficit Case . . . . .	42
4.5.6	Residual Deficit After Battery Dispatch . . . . .	43
4.5.7	Load-Shedding Response . . . . .	44
4.6	Short-Term EMS and Wind-Turbine Interaction . . . . .	44
4.6.1	Purpose and Operating Inputs of the Short-Term Case . . . . .	44
4.6.2	Wind-Side Operating Condition and Turbine Start-Up Response . . . . .	46
4.6.3	Reference and Simulated Wind-Turbine Power . . . . .	48
4.6.4	Battery Dispatch and SOC Evolution . . . . .	49
4.6.5	Mismatch Identification and Battery-Limited Residual Power . . . . .	51
4.6.6	Curtailment, Load Shedding, and Wind-Spill Transfer . . . . .	53
4.6.7	Blade-Pitch Response and Realised Wind-Power Reduction . . . . .	53

4.7	Key Result Values . . . . .	55
4.8	Integrated Interpretation . . . . .	55
4.9	Summary of Result Findings . . . . .	57
<b>5</b>	<b>Conclusion</b>	<b>59</b>
	<b>Bibliography</b>	<b>61</b>
<b>A</b>	<b>Supplementary Material</b>	<b>I</b>
A.1	Key Supervisory Variables . . . . .	I
A.2	Validation Structure Used in the Thesis . . . . .	II
A.3	Role of the Present Appendix . . . . .	II



# List of Figures

3.1	Overview of the inherited wind-turbine subsystem input connections.	21
3.2	Overview of the EMS and BESS interface connections. . . . .	22
3.3	Flowchart of the supervisory EMS logic. Battery action is prioritised before residual surplus or residual deficit is assigned to curtailment or load shedding. . . . .	22
3.4	Enlarged functional view of the implemented EMS signal structure, including renewable aggregation, battery-reference formation, battery dispatch, residual mismatch, wind-curtailment request, and load-shedding request. . . . .	24
3.5	Implemented battery-dispatch subsystem used to produce the constrained battery-power response from the EMS battery reference and SOC condition. . . . .	24
3.6	Implemented discharge branch of the BESS supervisory logic. . . . .	25
3.7	Implemented charge branch of the BESS supervisory logic. . . . .	25
3.8	Implemented wind-curtailment subsystem. The third input to the minimum operation is the realised simulated wind-turbine output $P_{\text{wind}}$ , consistent with the verified Simulink routing. . . . .	27
3.9	Connection of the EMS curtailment output to the inherited wind-spill path. The request $P_{\text{curt}}$ is passed as $P_{\text{spill}}$ , after which the inherited turbine-control dynamics determine the realised wind-power response.	28
3.10	Implemented load-shedding subsystem driven by residual deficit after battery action. . . . .	28
4.1	Long-term source and load profiles used as replay inputs for the EMS/BESS simulation. . . . .	36
4.2	Battery reference and constrained battery power in the long-term case.	37
4.3	Original deficit and surplus in the long-term case. . . . .	38
4.4	Simulated battery SOC in the long-term case. . . . .	38
4.5	Residual mismatch after battery action in the long-term case. . . . .	39
4.6	Curtailment and load-shedding requests in the long-term case. . . . .	40
4.7	Prescribed load profile in the deficit-validation case. . . . .	41
4.8	Original power deficit $P_{\text{deficit}}$ in the additional deficit validation case. . . . .	41
4.9	Constrained battery power $P_{\text{batt}}$ in the additional deficit validation case. Positive power corresponds to battery discharge and negative power corresponds to battery charging. . . . .	42
4.10	Simulated battery SOC in the additional deficit validation case. . . . .	43

4.11	Residual power deficit $P_{\text{deficit, res}}$ after constrained battery action in the additional deficit validation case. . . . .	43
4.12	Load-shedding request $P_{\text{loadshed}}$ generated in the additional deficit validation case. . . . .	44
4.13	Equivalent AC-side photovoltaic active-power input $P_{\text{pv}}$ in the short-term EMS simulation. . . . .	45
4.14	Prescribed load demand $P_{\text{load}}$ used as an EMS operating input in the 0–120 s short-term simulation. . . . .	45
4.15	Measured wind-speed condition in the short-term simulation. . . . .	46
4.16	Estimated wind-speed signal in the wind-turbine model. . . . .	47
4.17	Available wind-power estimate $P_{\text{wind, avail}}$ generated by the wind-turbine model during the 0–120 s short-term simulation. . . . .	47
4.18	Realised simulated wind-turbine output power $P_{\text{wind}}$ during the 0–120 s short-term simulation. . . . .	48
4.19	Reference and simulated wind-turbine output power. . . . .	48
4.20	Battery-power reference $P_{\text{batt, ref}}$ generated by the EMS during the 0–120 s short-term simulation. Positive power represents a discharge request and negative power represents a charging request. . . . .	49
4.21	Constrained battery power $P_{\text{batt}}$ during the 0–120 s short-term simulation. Positive power represents discharge and negative power represents charging. . . . .	50
4.22	Battery SOC in the short-term simulation. . . . .	50
4.23	Original power deficit $P_{\text{deficit}}$ before constrained battery action during the 0–120 s short-term simulation. . . . .	51
4.24	Original power surplus $P_{\text{surplus}}$ before constrained battery action during the 0–120 s short-term simulation. . . . .	51
4.25	Residual power deficit $P_{\text{deficit, res}}$ after constrained battery action during the 0–120 s short-term simulation. . . . .	52
4.26	Residual power surplus $P_{\text{surplus, res}}$ after constrained battery action during the 0–120 s short-term simulation. . . . .	52
4.27	EMS wind-power curtailment request $P_{\text{curt}}$ , supplied directly as the wind-spill command $P_{\text{spill}}$ during the 0–120 s short-term simulation. . . . .	53
4.28	Load-shedding request $P_{\text{loadshed}}$ during the 0–120 s short-term simulation. . . . .	54
4.29	Reference and simulated blade-pitch signals. . . . .	54

# List of Tables

3.1	Parameters of the implemented EMS/BESS supervisory operation. . .	26
3.2	Principal monitored variables in the implemented supervisory model.	29
4.1	Classification of signals used in the result analysis. . . . .	34
4.2	Parameters used in the result simulations. . . . .	35
4.3	Key numerical results from the presented simulations. . . . .	56



# 1

## Introduction

### 1.1 Background

The inherited wind-turbine model used in this thesis originates from the Chalmers wind-turbine installation at Björkö. The model and associated measurement-based signals provide the wind-side technical basis for the present EMS integration study. The transition towards low-carbon electricity systems has increased the use of renewable energy sources, distributed generation, and battery energy storage [1]. At the same time, microgrids have become an important framework for integrating local generation, storage, loads, and control functions within one coordinated electrical system [2, 3]. A microgrid may operate while connected to a larger network or may operate in islanded mode.

Islanded operation is particularly demanding because the external grid is no longer available to compensate for local power imbalance. Surplus generation cannot simply be exported, and insufficient generation cannot simply be supplied from the upstream grid. Instead, generation, storage, and demand must be coordinated locally. This challenge is especially relevant in systems combining wind and photovoltaic (PV) generation, since both sources depend on variable weather conditions [4, 5].

A battery energy storage system (BESS) can reduce the mismatch between renewable generation and load demand by charging during surplus conditions and discharging during deficit conditions. Nevertheless, battery operation is limited by charging power, discharging power, and state of charge (SOC). When these limits prevent the battery from fully balancing the system, further supervisory actions may be required. In the present thesis, these actions are wind-power curtailment in a residual-surplus condition and load shedding in a residual-deficit condition.

An Energy Management System (EMS) is therefore central to the system studied in this thesis. The EMS is treated as a supervisory active-power coordination layer. It determines the battery power request, evaluates whether the battery response is sufficient, and generates corrective-action requests when a remaining imbalance exists. The EMS is not intended to replace fast converter-level voltage or frequency control. Instead, it operates above the lower-level electrical control functions and coordinates the energy and active-power behaviour of the hybrid system.

The project brief defines the engineering problem in a consistent way. It states that islanded operation requires a proper balance between power production and power consumption. It also identifies battery storage as a balancing resource that should absorb surplus power or supply power during shortage, while load limitation may be required in an extreme deficit condition. Furthermore, the project brief treats the

grid-forming converter as an available lower-level element and places the thesis task on the control and coordination of the wind turbine, solar generation, and battery storage for smooth islanded operation [6]. The present thesis therefore focuses on supervisory power-balance control and system-level integration.

The technical starting point of the thesis is an inherited Chalmers wind-turbine model. This model provides wind-side behaviour that is relevant for islanded-operation analysis, including available wind-power estimation, wind-spill functionality, blade-angle response, and simulated wind-turbine output. Rather than reconstructing the wind-turbine subsystem, the present work extends the inherited model by adding a newly implemented EMS and a simplified BESS interface. This makes it possible to study how a supervisory power-balance controller interacts with the turbine-side wind-spill response.

A central distinction in the thesis is made between prescribed operating inputs and outputs produced by the implemented simulation structure. In the long-term EMS/BESS study, source and load profiles are supplied as replay inputs, while battery reference power, constrained battery power, SOC development, residual mismatch, curtailment request, and load-shedding request are generated by the developed EMS and BESS interface. In the short-term integrated study, the EMS curtailment request is connected to the inherited wind-spill input, allowing the associated blade-angle response and realised wind-turbine output to be examined within the inherited turbine model.

## 1.2 Literature Review and Research Gap

The literature relevant to this thesis can be grouped into four categories: microgrid control architecture, EMS design for hybrid renewable systems, simplified modelling for islanded-control studies, and previous Chalmers work related to the wind-turbine model used in this project.

### 1.2.1 Microgrid Control Architecture

Lasseter and Piagi [2] present the microgrid as a coordinated local power-system concept in which distributed resources and loads may be operated as an integrated entity. Their work establishes the system concept that underlies the present thesis: local generation, storage, and demand require a control structure when they are operated together.

Olivares et al. [3] review trends in microgrid control and distinguish among lower-level control functions, power-sharing functions, and higher-level energy-management functions. Their review is directly relevant to the present work because it supports the separation between converter-level electrical control and EMS-level active-power coordination.

Planas et al. [7] examine hierarchical controls and droop methods in microgrids. Palizban and Kauhaniemi [8] similarly review hierarchical control structures for distributed generation in islanded and grid-connected operation. Both studies show that islanded microgrids require coordinated layers of control rather than independent operation of individual sources and storage devices.

Tayab et al. [9] and De Brabandere et al. [10] focus more specifically on droop-based operation and power sharing among converter-interfaced units. These contributions are important for understanding the electrical-control background of islanded systems. However, they do not address the specific supervisory sequence studied here: mismatch calculation, constrained battery action, residual mismatch, and wind-spill-based curtailment.

The relevance of this group of studies to the present thesis is therefore mainly architectural. They justify the use of a supervisory EMS above lower-level electrical control, while the present thesis develops and evaluates the active-power coordination logic required for the specific wind–PV–battery system.

### 1.2.2 EMS Design for Hybrid Renewable Systems

Kumar et al. [11] study a small-scale hybrid wind–solar–battery microgrid and develop an EMS together with component and converter models. Their results demonstrate that battery action is essential for balancing varying renewable generation and demand in a hybrid system. This study is closely related to the present work in terms of the component combination considered. The present thesis differs by retaining an inherited wind-turbine model and by examining how a supervisory curtailment request is transferred into its wind-spill path.

Elkazaz et al. [12] propose a two-layer EMS for a PV–wind–battery microgrid. Their system uses convex programming together with model predictive and rolling-horizon predictive control, and the battery-control strategy is experimentally validated. Their contribution demonstrates the value of optimisation-based EMS design when economic operation and renewable self-consumption are primary objectives. In contrast, the present thesis uses a transparent power-balance-based supervisory structure, because its central objective is to trace the behaviour of the inherited wind-turbine model and the newly implemented BESS/EMS connection.

Zia et al. [13] develop and experimentally validate an EMS for an islanded DC microgrid containing PV, wind, tidal generation, and battery storage. Their study demonstrates how an optimised EMS can coordinate multiple renewable sources and battery storage in islanded operation. The present thesis shares the islanded balancing objective, but studies a different technical problem: the integration of an inherited Chalmers wind-turbine subsystem with a supervisory EMS whose wind-curtailment output is linked to a turbine-side wind-spill input.

Ely et al. [14] consider energy management in an autonomous wind–PV microgrid with battery storage. Their work supports the broader motivation for supervisory battery coordination in autonomous renewable systems. Together, these EMS studies establish that coordinated battery dispatch and renewable-power management are important for islanded hybrid operation.

The remaining issue for the present project is not whether an EMS is required, but how its outputs can be defined and interpreted transparently when it is connected to an existing dynamic wind-turbine model.

### 1.2.3 Simplified Models for Islanded-Control Evaluation

Zhang et al. [15] develop an energy-management strategy for an islanded microgrid based on power-flow control in a hybrid AC/DC configuration. Their work demonstrates that islanded operation can be coordinated through system-level active-power management rather than by considering each resource independently.

Bonfiglio et al. [16] propose a simplified microgrid model for the validation of islanded control logics. Their contribution is relevant to the modelling approach adopted in this thesis: a model need not reproduce every converter and network phenomenon in full detail when the research objective is to evaluate supervisory control logic in a structured and traceable manner.

These studies support the abstraction level used in the present work. PV generation and load demand are represented at supervisory active-power level, and the BESS is evaluated through power limitation and SOC development. Greater attention is retained for the inherited wind-turbine model because its wind-spill and blade-angle response are directly involved in the investigated curtailment mechanism.

### 1.2.4 Previous Chalmers Work and the Inherited Wind-Turbine Model

Previous Chalmers work provides the direct technical basis for this thesis. Eriksson [17] studies frequency control with wind power and addresses wind spilling and available-power-related behaviour in the context of the Chalmers wind turbine. This work is relevant because the present thesis uses an inherited wind-turbine modelling environment containing a wind-spill path and available wind-power information.

Mal and Bukhari [18] study islanded operation of a wind turbine with solar power and battery storage in MATLAB/Simulink. Their work establishes the closest system-level context for the current project: an islanded hybrid system combining wind generation, PV generation, battery storage, and load demand. It also demonstrates the relevance of the Chalmers wind-turbine setting for such a hybrid-system study.

The present thesis builds on this starting point by introducing an explicit power-balance-oriented EMS and a simplified BESS interface. The implemented EMS generates battery and corrective-action variables that are separately observable in simulation. The key EMS-related output variables are presented as follows:

$P_{\text{batt,ref}}$ ,  $P_{\text{batt}}$ ,  $P_{\text{deficit}}$ ,  $P_{\text{surplus}}$ ,  $P_{\text{deficit,res}}$ ,  $P_{\text{surplus,res}}$ ,  $P_{\text{curt}}$ , and  $P_{\text{loadshed}}$ .

For the wind-curtailment path, the EMS output is connected to the inherited wind-turbine model through

$$P_{\text{spill}} = P_{\text{curt}}. \quad (1.1)$$

This connection enables the curtailment request to be evaluated through the blade-angle response and the resulting realised wind-turbine output, rather than being interpreted only as a numerical power reduction.

### 1.2.5 Research Gap Addressed in This Thesis

The reviewed studies establish several important principles. Microgrid-control literature explains why islanded systems require hierarchical coordination. Hybrid renewable EMS studies demonstrate the role of battery storage and supervisory dispatch. Simplified modelling studies show that control logic can be evaluated without reproducing every lower-level component in full detail. Previous Chalmers work provides the wind-turbine modelling basis and the direct islanded-operation context.

Nevertheless, a specific integration issue remains. The reviewed EMS studies do not examine the use of the inherited Chalmers wind-spill input as the execution path for a supervisory curtailment command. Conversely, the earlier Chalmers work does not formulate the same explicit EMS structure in which initial mismatch, constrained battery action, residual mismatch, curtailment request, and load-shedding request are separately calculated and interpreted.

The present thesis addresses this gap by integrating a power-balance-oriented EMS and a simplified BESS interface with the inherited wind-turbine model. The contribution is organised around three aspects.

First, the thesis separates the wind-power availability signal from the wind power delivered by the simulated turbine. These two signals are denoted as  $P_{\text{wind,avail}}$  and  $P_{\text{wind}}$ , respectively. The former is used as an available-power reference, while the latter is interpreted as the realised wind-turbine output.

Second, the EMS represents battery action and remaining imbalance through an explicit sequence consisting of the battery reference, constrained battery power, and residual surplus or deficit.

Third, the EMS wind-curtailment request is supplied to the inherited wind-spill path. The resulting blade-angle response and realised wind-power reduction are then analysed as wind-turbine-side simulation outputs.

In addition, the thesis clearly distinguishes replayed operating profiles used as simulation inputs from the EMS/BESS variables generated as simulation outputs. This distinction is particularly important in the long-term analysis, where the objective is to demonstrate the response of the newly implemented EMS and BESS structure to time-varying operating profiles.

## 1.3 Aim and Scope

The aim of this thesis is to develop and evaluate a supervisory simulation framework for the islanded operation of a hybrid system consisting of a wind turbine, PV generation, battery storage, and electrical load. The central focus is active-power balance and the coordination of battery action, wind curtailment, and load shedding under variable operating conditions.

The specific objectives are:

1. to integrate an inherited wind-turbine model with a newly implemented supervisory EMS and a simplified BESS interface;
2. to formulate a transparent active-power-balance structure for coordinating wind power, PV power, battery storage, SOC, and load demand;

3. to distinguish initial renewable-load mismatch from the residual mismatch remaining after constrained battery action;
4. to generate wind-curtailment and load-shedding requests from residual surplus and residual deficit, respectively;
5. to connect the wind-curtailment request to the inherited wind-spill path and examine the associated blade-angle and wind-power response;
6. to evaluate the EMS/BESS behaviour over a long-term operating profile and the EMS-wind-turbine interaction over a short-term dynamic interval.

In accordance with the project brief, the grid-forming converter is treated as a lower-level element, while the main contribution of this thesis concerns supervisory active-power coordination [6]. This scope is consistent with the hierarchical separation between supervisory energy management and lower-level electrical control discussed in the microgrid literature [3, 8, 7].

## 1.4 Research Questions

The thesis addresses the following research questions:

1. How can an islanded wind-PV-battery system be represented in Simulink with a transparent supervisory active-power-balance structure?
2. How can battery charge and discharge action be coordinated under battery power constraints and SOC conditions?
3. How can remaining surplus and deficit after battery action be identified and translated into curtailment and load-shedding requests?
4. How can a supervisory wind-curtailment request be applied through the inherited wind-spill path and evaluated through blade-angle and realised wind-power behaviour?
5. How can replayed input profiles be clearly separated from outputs generated by the implemented EMS, BESS interface, and inherited wind-turbine model?

## 1.5 Scientific and Engineering Contribution

The main contribution of this thesis is the development of a traceable supervisory EMS structure around an inherited dynamic wind-turbine model. The work does not treat the wind turbine as a simple algebraic power source. Instead, it retains the turbine-side response associated with wind spilling and blade-angle variation.

The thesis contributes by:

- integrating the inherited wind-turbine subsystem with a supervisory EMS and a simplified BESS interface;
- distinguishing the available wind-power estimate from the realised simulated wind-turbine output;
- implementing observable battery-reference, battery-response, mismatch, and residual-mismatch variables;
- generating curtailment and load-shedding requests from the residual mismatch after battery action;

- connecting the EMS curtailment output to the inherited wind-spill input and analysing the resulting blade-angle and wind-power behaviour;
- distinguishing simulation inputs from EMS/BESS and wind-turbine simulation outputs in the interpretation of the results.

The long-term EMS/BESS simulation evaluates how time-varying operating profiles are processed by the supervisory controller and battery representation. The short-term integrated simulation evaluates how the EMS curtailment request interacts with the inherited wind-turbine subsystem. Together, these analyses provide evidence for the developed supervisory coordination structure in the islanded hybrid-system context.

## 1.6 Methodological Overview

The thesis adopts a layered modelling strategy. The inherited wind-turbine model is retained as the wind-side technical basis. PV generation and load demand are represented by active-power signals appropriate for EMS-level analysis. A simplified BESS interface supplies the relationship between battery action and SOC development. The EMS is added as the supervisory layer that coordinates the power balance among these elements.

At supervisory level, the EMS receives wind-power information, PV power, load demand, and SOC. It generates the battery reference, constrained battery power, residual mismatch, curtailment request, and load-shedding request. For the short-term integrated analysis, the curtailment request is supplied to the inherited wind-spill input so that the turbine-side response can be studied.

The two simulation time scales serve different purposes. The long-term study is used to evaluate EMS/BESS operation over an extended profile. The short-term study is used to evaluate the wind-spill and blade-angle-related response during a selected dynamic interval. This organisation separates the supervisory balancing evidence from the turbine-side dynamic interaction evidence.

## 1.7 Thesis Structure

The remainder of the thesis is organised as follows. Chapter 2 presents the theoretical and modelling background of islanded hybrid power systems, wind power, PV power, battery storage, supervisory power balance, wind curtailment, and load shedding. Chapter 3 describes the MATLAB/Simulink implementation, including the inherited wind-turbine subsystem, the EMS, the simplified BESS interface, and the wind-spill connection. Chapter 4 presents the simulation results by first examining long-term EMS/BESS behaviour and then analysing the short-term EMS–wind-turbine interaction. Chapter 5 concludes the thesis and identifies directions for further development.



# 2

## Theory and Modelling Background

### 2.1 Islanded Hybrid Power Systems

An islanded hybrid power system is a local electric power system, and it works without continuous support from a larger transmission or distribution grid. In this kind of system, local generation, local storage, and local load demand have to be balanced inside the system itself. This is different from grid-connected operation, because in grid-connected operation the main grid can provide a strong reference for voltage, frequency, and power balance over short time periods.

Islanded hybrid systems are relevant when local renewable integration, resilience, and energy autonomy are important. A typical configuration includes renewable energy sources, a battery energy storage system, local loads, and a supervisory control layer that coordinates source, storage, and demand-side actions. The main challenge is that renewable generation, especially wind and photovoltaic generation, is variable and only partially controllable. Therefore, smooth islanded operation requires more than generation availability; it requires coordinated active-power management [3, 8, 7].

From an active-power perspective, the basic operating requirement of an islanded system can be written as

$$\sum P_{\text{gen}} + \sum P_{\text{storage}} = \sum P_{\text{load}} + P_{\text{loss}}, \quad (2.1)$$

where  $\sum P_{\text{gen}}$  denotes the total contribution from generation units,  $\sum P_{\text{storage}}$  denotes the net contribution from storage, and  $\sum P_{\text{load}}$  denotes the total demand. The term  $P_{\text{loss}}$  denotes aggregated electrical and conversion losses that may occur in a physical islanded system, including losses associated with local power transfer, power-electronic conversion, and battery power exchange. This term is included here only for the general system-level power balance. In the supervisory EMS model developed in this thesis, losses are not used as a separate dynamic input signal; instead, the implemented balance is calculated from the active-power signals that are given to the model or produced by the model.

In the general expression in Equation (2.1),  $\sum P_{\text{gen}}$  is a generic generation term. In the implemented wind–PV system studied in this thesis, no additional dispatchable generator is represented. The generation quantity used in the EMS is therefore the aggregated renewable power  $P_{\text{ren}}$ , defined later as the sum of realised wind-turbine output and photovoltaic contribution. Within the implemented modelling scope,  $\sum P_{\text{gen}}$  is represented by  $P_{\text{ren}}$ .

Although the balance in Equation (2.1) is simple in form, maintaining it in real time

becomes difficult when generation sources are weather-dependent and the battery is constrained by both power and energy limits.

In the project studied in this thesis, the system includes a wind turbine, photovoltaic generation, a battery energy storage system, and a local load. The battery works as a local balancing unit. It discharges when there is a power deficit, and it charges when there is surplus power. If the battery cannot remove the whole mismatch by itself, other supervisory actions may be needed, such as wind curtailment or load shedding. This system-level interpretation is consistent with the project specification for the Chalmers island-operation study [6].

## 2.2 Operational Challenges in Islanded Mode

The main difficulty in islanded operation is that changes in load or renewable generation need to be handled locally. In a large interconnected power system, small local mismatches can be absorbed by the external grid; however, in an islanded system, the local sources, local storage, and local control have to provide the balancing capability by themselves.

In converter-based islanded systems, fast voltage and frequency control is normally handled at the converter-control level. The EMS used in this thesis is not meant to replace this fast control; instead, it works as a slower supervisory layer for active-power coordination. Its task is to decide how much power should be requested from the battery, whether wind power needs to be curtailed, and whether load shedding is needed under constrained operating conditions. This separation between lower-level electrical control and higher-level supervisory coordination follows the hierarchical microgrid control structures discussed in the literature [3, 8, 7].

The active-power mismatch can be expressed conceptually as

$$\Delta P = P_{\text{gen}} + P_{\text{storage}} - P_{\text{load}} - P_{\text{loss}}. \quad (2.2)$$

A positive or negative mismatch means that the local sources, storage, and load are not balanced in active power. In a converter-formed islanded grid, the exact frequency response is related to the converter-control strategy; therefore, frequency behaviour is only used as background motivation in this thesis, while the implemented EMS mainly deals with the active-power allocation problem.

The supervisory control problem can be summarized through four practical questions:

- How much wind and PV power is available?
- How much renewable power is actually delivered to the local balance?
- Can the battery absorb or supply the mismatch within its power and SOC constraints?
- Does any residual surplus or residual deficit require curtailment or load shedding?

These questions are connected with each other. For example, the battery may have enough instantaneous power capability, but it may still not be allowed to discharge when the SOC is close to the lower operating threshold. In a similar way, renewable curtailment may be needed when the battery cannot absorb more surplus power.

Therefore, the EMS has to make coordinated decisions according to the source condition, the storage state, and the load demand.

### 2.3 Supervisory Control Scope and Modelling Boundary

The present thesis focuses on supervisory active-power coordination rather than detailed converter-control design. This boundary is important for interpreting both the model implementation and the simulation results. In a physical islanded installation, lower-level converter control is required to establish and regulate the electrical operating conditions of the local grid. In the Björkö-related project context, the grid-forming converter and battery equipment are treated as the lower-level execution layer, while the thesis task concerns the coordination of wind power, PV power, battery support, and load demand [6].

Based on this modelling boundary, the EMS developed in this thesis is not used to reproduce fast voltage or frequency regulation dynamics. Its main function is to assign active-power balancing actions at the supervisory level. The EMS receives the realised wind-turbine output, the equivalent photovoltaic active-power contribution, the load demand, and the battery state information; after that, it decides the battery-power request and checks whether the remaining surplus or deficit should lead to wind curtailment or load shedding.

This scope is consistent with the hierarchical interpretation of microgrid control used in the literature, where supervisory energy-management functions are distinguished from faster device-level and converter-level control functions [3, 8, 7]. The theory presented in the following sections therefore concentrates on the power quantities and corrective actions that are directly implemented and evaluated in the thesis.

### 2.4 Wind-Turbine Power Background

Wind energy conversion is governed by aerodynamic power capture, rotor dynamics, electromechanical conversion, and turbine control. The aerodynamic power available from the wind is commonly expressed as [17]

$$P_{\text{wind,mech}} = \frac{1}{2} \rho A v^3 C_p(\lambda, \beta), \quad (2.3)$$

where  $\rho$  is the air density,  $A$  is the rotor swept area,  $v$  is the wind speed,  $C_p$  is the power coefficient,  $\lambda$  is the tip-speed ratio, and  $\beta$  is the blade-pitch angle.

The tip-speed ratio is defined as [17]

$$\lambda = \frac{\omega_r R}{v}, \quad (2.4)$$

where  $\omega_r$  is the rotor angular speed and  $R$  is the rotor radius. These equations show that wind power depends not only on the wind speed itself, but also on turbine operating conditions. Blade-pitch angle, rotor speed, and control actions can change

how much of the available aerodynamic power is converted into delivered electrical power.

For this reason, a distinction is made between available wind power and realised wind-turbine output:

- *available wind power*, denoted by  $P_{\text{wind,avail}}$ , is the rated-power-capped wind-side availability estimate produced by the inherited wind model;
- *realised wind-turbine output*, denoted by  $P_{\text{wind}}$ , is the simulated wind power delivered after the inherited turbine dynamics and, when activated, the wind-spill and pitch-control response.

This distinction is important in this thesis. The available wind-power estimate is kept as a wind-side reference, which is used to interpret the turbine operation and the reduction of realised power. It is not used as the limiting input in the developed Wind Curtailment subsystem. According to the checked Simulink signal routing, the realised simulated wind-turbine output  $P_{\text{wind}}$  is used in two places: it is used in the supervisory power-balance calculation, and it is also used as the wind-power limiting input in the implemented curtailment block.

The spilling-power request is realised through the blade-pitch response and the turbine-controller response. This treatment follows the inherited Chalmers wind model, where wind spilling is obtained by adjusting turbine-control quantities, rather than by deleting power numerically after the simulation [17].

## 2.5 Photovoltaic Power Representation

Photovoltaic generation changes solar irradiance into electrical power through semiconductor devices and power electronic interfaces. A detailed PV model may include irradiance, temperature, current-voltage characteristics, maximum power point tracking, DC-link dynamics, and converter control. In this thesis, the PV contribution is only represented at the supervisory level as an active-power input:

$$P_{\text{pv}} = P_{\text{pv,avail}}. \quad (2.5)$$

In the implemented supervisory model,  $P_{\text{pv}}$  is interpreted as the equivalent AC-side active-power contribution available at the EMS power-balance interface. The detailed DC-side PV-panel output, DC-link behaviour, and inverter conversion dynamics are not separately represented in the implemented model. Consequently,  $P_{\text{pv}}$  should not be interpreted as a measured DC panel-output variable; it represents the photovoltaic power contribution made available to the islanded active-power balance after an unmodelled PV conversion interface.

This modelling choice follows the purpose of the EMS study. The PV subsystem gives an active-power signal to the supervisory balance, while the main work in this thesis focuses on the coordination among renewable power, battery storage, load demand, curtailment, and load shedding. Using PV active-power signals in a supervisory hybrid wind-PV-battery control context is also consistent with previous islanded-system studies at Chalmers [18].

## 2.6 Battery Energy Storage in Islanded Operation

Battery energy storage is an important balancing part in islanded renewable systems. Different from wind and solar generation, the battery can be controlled within its technical limits. When local generation is not enough, the battery can discharge to supply power; when renewable generation is higher than the load demand, the battery can charge and absorb part of the surplus power. In hybrid renewable microgrids, this storage action is usually coordinated by an EMS, together with the source condition and the load condition [11].

At supervisory level, the battery representation must account for at least the following quantities:

- maximum discharging power magnitude  $P_{\text{dis,max}}$ ;
- maximum charging power magnitude  $P_{\text{ch,max}}$ ;
- lower state-of-charge threshold  $SOC_{\text{min}}$ ;
- upper state-of-charge threshold  $SOC_{\text{max}}$ .

Using the sign convention adopted in this thesis, positive battery power denotes discharge and negative battery power denotes charge. For the simplified BESS interface adopted in this thesis, the SOC evolution is represented at energy level as

$$SOC(t) = SOC(t_0) - \frac{1}{E_{\text{nom}}} \int_{t_0}^t P_{\text{batt}}(\tau) d\tau, \quad (2.6)$$

where  $E_{\text{nom}}$  is the nominal stored energy. With this sign convention, sustained positive  $P_{\text{batt}}$  reduces SOC, while sustained negative  $P_{\text{batt}}$  increases SOC.

Equation (2.6) defines the supervisory energy-level representation used for interpretation. The implementation chapter documents the current-based form applied in the Simulink BESS interface.

## 2.7 Energy Management System as a Supervisory Layer

The EMS is used as the supervisory control layer in this thesis, and it coordinates the relation among renewable sources, storage, and load. It works mainly with active-power and SOC variables, not with low-level converter switching variables. This kind of separation between an energy-management layer and a device-control layer is also often used in microgrid control studies [3, 8, 11].

In the present thesis, the EMS determines:

- the battery-power reference;
- the constrained battery power after power and SOC limitations;
- the original deficit and surplus components;
- the residual deficit and surplus after battery action;
- the wind-curtailment request;
- the load-shedding request.

Therefore, the EMS works as a coordination layer, and it sends power commands that can be interpreted by the component and interface models. This also fits the main contribution of the thesis, which is the system integration and supervisory power-balance logic around the inherited wind-turbine subsystem.

## 2.8 Supervisory Power-Balance Formulation

The starting point of the implemented EMS logic is the renewable power used for the instantaneous active-power balance. In the integrated simulation, the realised wind-turbine output is used, because the battery and load-side decisions need to follow the wind power that is actually delivered by the inherited wind model:

$$P_{\text{ren}} = P_{\text{wind}} + P_{\text{pv}}. \quad (2.7)$$

The available wind-power estimate  $P_{\text{wind,avail}}$  is treated separately as a wind-side availability reference. It is used to interpret the difference between available and realised wind power during turbine-side curtailment, but it does not replace  $P_{\text{wind}}$  in the instantaneous EMS power-balance calculation.

Before battery constraints are applied, the desired battery reference is calculated as

$$P_{\text{batt,ref}} = P_{\text{load}} - P_{\text{ren}}. \quad (2.8)$$

With the adopted sign convention:

- $P_{\text{batt,ref}} > 0$  requests battery discharge;
- $P_{\text{batt,ref}} < 0$  requests battery charging.

The original mismatch is separated into non-negative deficit and surplus components:

$$P_{\text{deficit}} = \max(P_{\text{batt,ref}}, 0), \quad (2.9)$$

$$P_{\text{surplus}} = \max(-P_{\text{batt,ref}}, 0). \quad (2.10)$$

This separation makes it possible to distinguish the initial renewable-load mismatch from the imbalance that may still remain after the battery constraints have been applied.

## 2.9 Battery Constraint Logic

The final battery power cannot always equal the unconstrained reference  $P_{\text{batt,ref}}$ . It must satisfy charging-power, discharging-power, and SOC constraints. A rule-based representation of the implemented supervisory logic is

$$P_{\text{batt}} = \begin{cases} \min(P_{\text{batt,ref}}, P_{\text{dis,max}}), & P_{\text{batt,ref}} > 0, \text{ SOC} > \text{SOC}_{\text{min}}, \\ \max(P_{\text{batt,ref}}, -P_{\text{ch,max}}), & P_{\text{batt,ref}} < 0, \text{ SOC} < \text{SOC}_{\text{max}}, \\ 0, & \text{otherwise.} \end{cases} \quad (2.11)$$

Here,  $P_{\text{ch,max}}$  is defined as a positive charging-power magnitude. Accordingly, with a 5 kW charging limit and the sign convention used in this thesis, the minimum charging power appearing in the battery signal is  $-P_{\text{ch,max}} = -5$  kW.

## 2.10 Residual Mismatch and Corrective Actions

After the constrained battery power has been determined, the remaining mismatch is calculated as

$$P_{\text{err}} = P_{\text{batt,ref}} - P_{\text{batt}}. \quad (2.12)$$

The residual mismatch is separated into residual deficit and residual surplus:

$$P_{\text{deficit,res}} = \max(P_{\text{err}}, 0), \quad (2.13)$$

$$P_{\text{surplus,res}} = \max(-P_{\text{err}}, 0). \quad (2.14)$$

The residual quantities define whether secondary corrective action is required:

- if  $P_{\text{surplus,res}} > 0$ , wind curtailment is requested;
- if  $P_{\text{deficit,res}} > 0$ , load shedding is requested.

This two-stage structure is important for explaining the results. The original mismatch shows the system condition before the battery takes action, while the residual mismatch shows the part that is still not balanced after the possible battery action has been applied.

## 2.11 Wind Curtailment and Load Shedding

Curtailment and load shedding are used as corrective actions after the feasible battery response has already been decided. For this reason, they are not used as the first balancing method in the EMS hierarchy.

### 2.11.1 Wind Curtailment

Wind curtailment is activated when residual surplus remains after battery charging has been limited. In accordance with the verified input routing of the implemented Wind Curtailment subsystem, its wind-side limiting input is the realised simulated wind-turbine output  $P_{\text{wind}}$ . The implemented curtailment request is therefore represented as

$$P_{\text{curt}} = \min(P_{\text{surplus,res}}, P_{\text{wind}}). \quad (2.15)$$

The available wind-power estimate  $P_{\text{wind,avail}}$  remains useful as an interpretation reference for the wind-side operating condition, but it is not written as the signal entering the implemented curtailment minimum block.

In this thesis, curtailment is not implemented as direct algebraic subtraction from the wind-power signal. Instead, the EMS curtailment request is passed to the inherited wind-spill path:

$$P_{\text{spill}} = P_{\text{curt}}. \quad (2.16)$$

The inherited wind-spill and pitch-control mechanism then determines the simulated blade-pitch response and resulting realised wind-turbine output. Accordingly, a residual surplus first produces the EMS curtailment request. Through the assignment  $P_{\text{spill}} = P_{\text{curt}}$ , this request is passed to the inherited turbine-control path, whose blade-pitch response determines the resulting realised wind-turbine output  $P_{\text{wind}}$ . This turbine-side interpretation is consistent with the inherited Chalmers wind model documented in [17].

### 2.11.2 Load Shedding

Load shedding is activated when a residual deficit is still left after the allowable battery discharge. The shed-load request is denoted as  $P_{\text{loadshed}}$ , and the effective load is

$$P_{\text{load,eff}} = P_{\text{load}} - P_{\text{loadshed}}. \quad (2.17)$$

In the EMS hierarchy, load shedding is used as the last corrective action. It is only activated when the realised renewable generation and the allowable battery discharge are still not enough to cover the original load demand; this follows the project requirement for shortage operation [6].

## 2.12 Corrected Power Variables and Interface Logic

A key modelling decision in this thesis is to separate available variables, realised variables, and corrected downstream variables. Available variables describe source availability or original demand, while realised variables describe outputs after component dynamics and control actions. Corrected downstream variables are the quantities passed to the downstream power-balance interpretation after the EMS decisions are applied.

The corrected wind-side contribution is defined as

$$P_{\text{wind,down}} = P_{\text{wind}}. \quad (2.18)$$

Wind curtailment is not subtracted again downstream because the curtailment request has already entered the inherited wind-spill and pitch-control path.

The remaining corrected variables are

$$P_{\text{load,eff}} = P_{\text{load}} - P_{\text{loadshed}}, \quad (2.19)$$

$$P_{\text{pv,eff}} = P_{\text{pv}}, \quad (2.20)$$

$$P_{\text{batt,eff}} = P_{\text{batt}}. \quad (2.21)$$

The net-power expression used for downstream active-power interpretation is

$$P_{\text{net}} = P_{\text{load,eff}} - P_{\text{wind}} - P_{\text{pv,eff}} - P_{\text{batt,eff}}. \quad (2.22)$$

In an ideally balanced supervisory operating condition,

$$P_{\text{net}} \approx 0. \quad (2.23)$$

This expression gives a consistent link between the EMS decisions and the downstream power-balance interpretation. It also helps avoid double counting; the shed load is not still treated as supplied demand, and wind curtailment is not subtracted again after the wind model has already produced its realised response.

## 2.13 Hierarchical Modelling Philosophy

The modelling approach used in this thesis is hierarchical. The inherited wind-turbine model gives the turbine-side dynamics and the wind-spill and pitch response. The PV and load are represented as active-power signals, which is suitable for EMS-level studies. The BESS interface gives the constrained battery power and the SOC evolution. Above these component or interface parts, the EMS is used to coordinate the active-power balance.

The hierarchy can be summarized as:

1. **source and component layer:** wind turbine, PV representation, battery representation, and load;
2. **supervisory layer:** EMS logic for battery dispatch, curtailment, and load shedding;
3. **system interaction layer:** corrected power variables and downstream active-power interpretation.

This layered organisation is consistent with hierarchical microgrid-control thinking [3, 8, 7]. It is suitable for this thesis, because the main contribution is to connect the inherited wind-turbine model with a broader islanded hybrid power-system framework by using explicit supervisory control logic.

## 2.14 Modelling Scope of the Theory

The theoretical framework in this chapter is focused on supervisory active-power coordination. It gives the concepts needed for the implementation chapter, including realised renewable power, available wind-power reference, battery-reference generation, battery feasibility constraints, residual mismatch, curtailment, load shedding, and corrected downstream power variables.

Within this modelling scope, the PV source is represented as an EMS-level active-power input, the battery is represented by power limits and SOC evolution, and the inherited wind model gives the wind-side availability and realised output signals. This level of abstraction is used because the thesis evaluates the supervisory coordination of an islanded wind-solar-battery system, rather than the detailed internal design of each device controller.

The EMS first evaluates the renewable-load mismatch by using the realised wind-turbine output and PV power. It then applies the battery constraints, calculates the residual mismatch, and activates wind curtailment or load shedding when they are needed. The available wind power is kept as a wind-side reference for interpretation, while the realised wind-turbine output is used both as the delivered wind contribution and as the wind-side signal in the implemented curtailment limitation.



# 3

## Methods and Implementation

### 3.1 Overall Modelling Strategy

In this thesis, a layered modelling strategy in MATLAB/Simulink is used to study islanded operation with wind power, photovoltaic generation, battery storage, and local load demand. The implementation is mainly used to evaluate a supervisory active-power management structure; it does not try to rebuild all component models from the converter-switching level or the electromagnetic level.

The wind-turbine subsystem used in the thesis is inherited from previously developed Chalmers model material. It provides the wind-side dynamic behaviour, including wind-speed-related processing, available-power estimation, turbine rotational-speed behaviour, the wind-spill path, and the blade-pitch response [17, 18]. The newly developed work in this thesis is the supervisory integration around this inherited wind model: the Energy Management System (EMS), the simplified Battery Energy Storage System (BESS) interface, the residual-mismatch processing, the curtailment and load-shedding commands, and the connection of the EMS curtailment output to the inherited wind-spill input.

The complete modelling structure is divided into three functional layers:

1. a **source and storage layer**, consisting of the inherited wind-turbine subsystem, the equivalent AC-side PV active-power input, the BESS interface, and the load representation;
2. a **supervisory EMS layer**, which evaluates the renewable-load mismatch, requests battery action, identifies residual imbalance, and issues curtailment or load-shedding commands;
3. an **interface and monitoring layer**, which provides the corrected system-level variables used for interpreting the simulation results.

This modelling strategy separates the inherited component-level wind-turbine behaviour from the supervisory controller developed in this thesis. It also helps to make a distinction between the input profiles and the outputs generated by the model. In the long-term EMS/BESS simulation, the time-varying wind, PV, and load profiles are given to the developed supervisory structure; the battery-reference power, constrained battery power, SOC evolution, residual mismatch, curtailment request, and load-shedding request are then produced by the implemented model. In the short-term integrated simulation, the EMS curtailment request is connected to the inherited wind-spill path, so the resulting blade-pitch response and wind-turbine power response can be evaluated.

## 3.2 Simulation Environment and Modelling Boundary

The implementation is carried out in MATLAB/Simulink. Simulink is suitable for this work, because the EMS can be represented by signal routing, subsystem structures, saturation blocks, logical conditions, and monitored internal variables. The implemented model mainly works with active-power signals and storage-state signals:

$$\{P_{\text{wind}}, P_{\text{wind,avail}}, P_{\text{pv}}, P_{\text{load}}, P_{\text{batt,ref}}, P_{\text{batt}}, P_{\text{curt}}, P_{\text{loadshed}}, SOC\}. \quad (3.1)$$

The modelling boundary in this work is at the supervisory level. The EMS is used to determine active-power commands and corrective actions for islanded operation. The dynamic response of the wind turbine is given by the inherited wind model, while the BESS is described through a system-level interface, which produces the battery-power response and the SOC trajectory. This boundary also follows the project specification; the grid-forming converter and the battery equipment are treated as the lower-level electrical execution part, while this thesis mainly develops and evaluates the supervisory coordination of the local sources, storage, and demand [6].

Within this modelling boundary,  $P_{\text{pv}}$  is supplied to the EMS as an equivalent AC-side photovoltaic active-power contribution at the power-balance interface. The PV-panel DC-side behaviour and inverter conversion dynamics are not separately implemented. This definition ensures that  $P_{\text{pv}}$  is interpreted consistently with the active-power balance evaluated by the EMS.

## 3.3 Inherited Wind-Turbine Subsystem

The inherited wind-turbine subsystem is used as the wind-side dynamic model in the integrated simulation. Its role in this thesis is to provide a realised wind-turbine power response and to execute the wind-spill action requested by the EMS.

Two wind-related power variables are retained because they have different modelling meanings:

- $P_{\text{wind,avail}}$  is the available wind-power estimate generated by the inherited wind-side model and limited by its rated-power cap. It is retained as an availability reference for interpreting the turbine operating condition;
- $P_{\text{wind}}$  is the realised simulated wind-turbine output after the inherited turbine dynamics and, when activated, the wind-spill and blade-pitch response.

In the implemented model verified for this thesis,  $P_{\text{wind}}$  is the wind-power signal routed into the supervisory renewable aggregation and into the developed Wind Curtailment subsystem. Accordingly, this chapter documents  $P_{\text{wind}}$ , not  $P_{\text{wind,avail}}$ , as the wind-side limiting signal used by the implemented curtailment block.

Figure 3.1 identifies the external input connections used when integrating the inherited wind-turbine subsystem with the developed supervisory structure. The internal inherited subsystem is not re-derived in this thesis; it is integrated with the EMS through the wind-power and spilling-power signals.

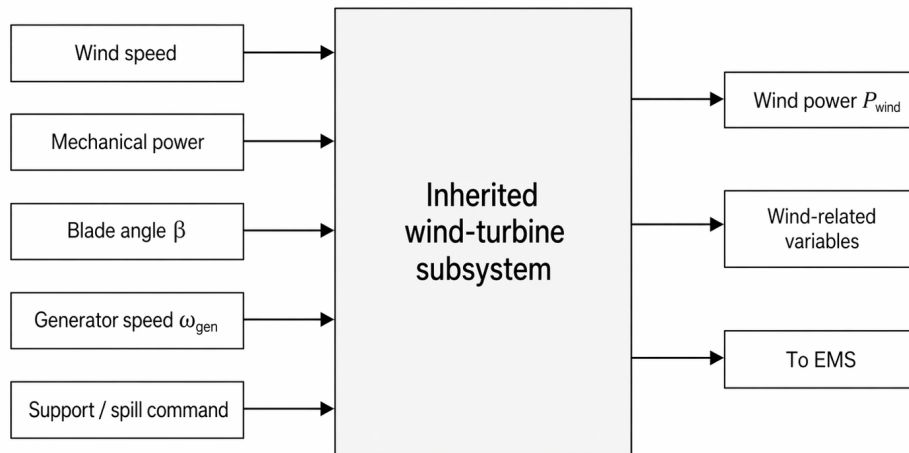


**Figure 3.1:** Overview of the inherited wind-turbine subsystem input connections.

### 3.4 EMS–BESS–Interface Architecture

The developed supervisory structure receives wind power, equivalent AC-side PV active power, load demand, and battery SOC information. It generates the battery-power reference, the constrained battery response, the original and residual mismatch indicators, and the corrective outputs for curtailment and load shedding.

The source and load signals define the instantaneous active-power condition. The EMS first generates a battery reference. The BESS interface then applies the allowable storage response and provides the resulting battery power and SOC behaviour. When the battery response does not remove the remaining imbalance, the EMS activates a corrective request: wind curtailment for residual surplus or load shedding for residual deficit.

This representation also makes the status of the long-term simulation outputs explicit. Profiles supplied at the input side of the functional structure are operating conditions. Signals such as  $P_{\text{batt,ref}}$ ,  $P_{\text{batt}}$ ,  $P_{\text{deficit,res}}$ ,  $P_{\text{surplus,res}}$ ,  $P_{\text{curt}}$ ,  $P_{\text{loadshed}}$ , and the simulated *SOC* trajectory are generated within the developed EMS/BESS implementation.

### 3.5 Supervisory Control Sequence

The supervisory control logic is organised as a priority-based sequence. The battery is used as the first controllable balancing resource after the renewable and load condition has been evaluated. Curtailment and load shedding are used only after the constrained battery response has been determined.

Figure 3.3 presents the supervisory decision logic implemented in the EMS. The flowchart starts from the measured or prescribed operating inputs used by the EMS: the realised wind-turbine output  $P_{\text{wind}}$ , the equivalent PV active-power contribution

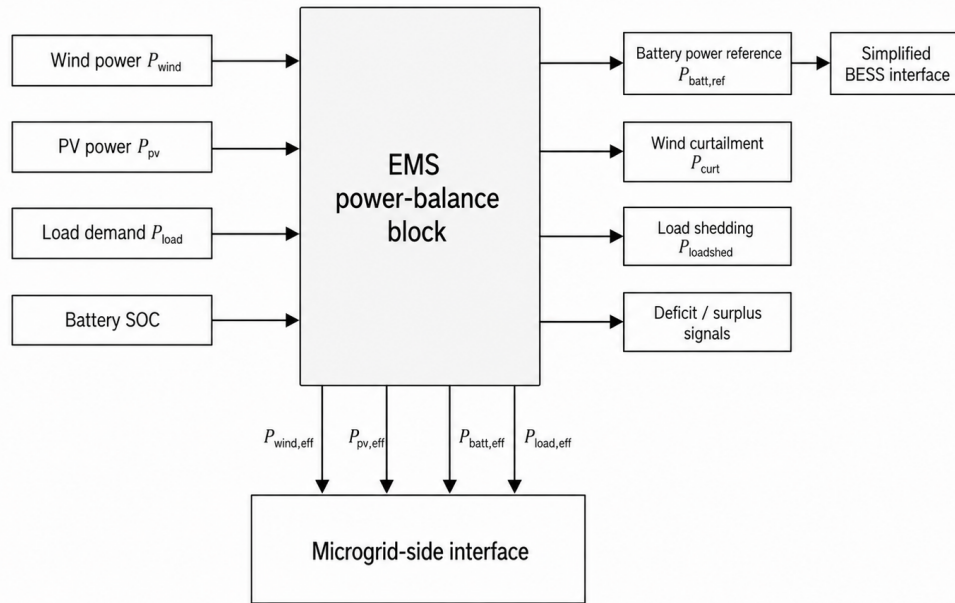


Figure 3.2: Overview of the EMS and BESS interface connections.

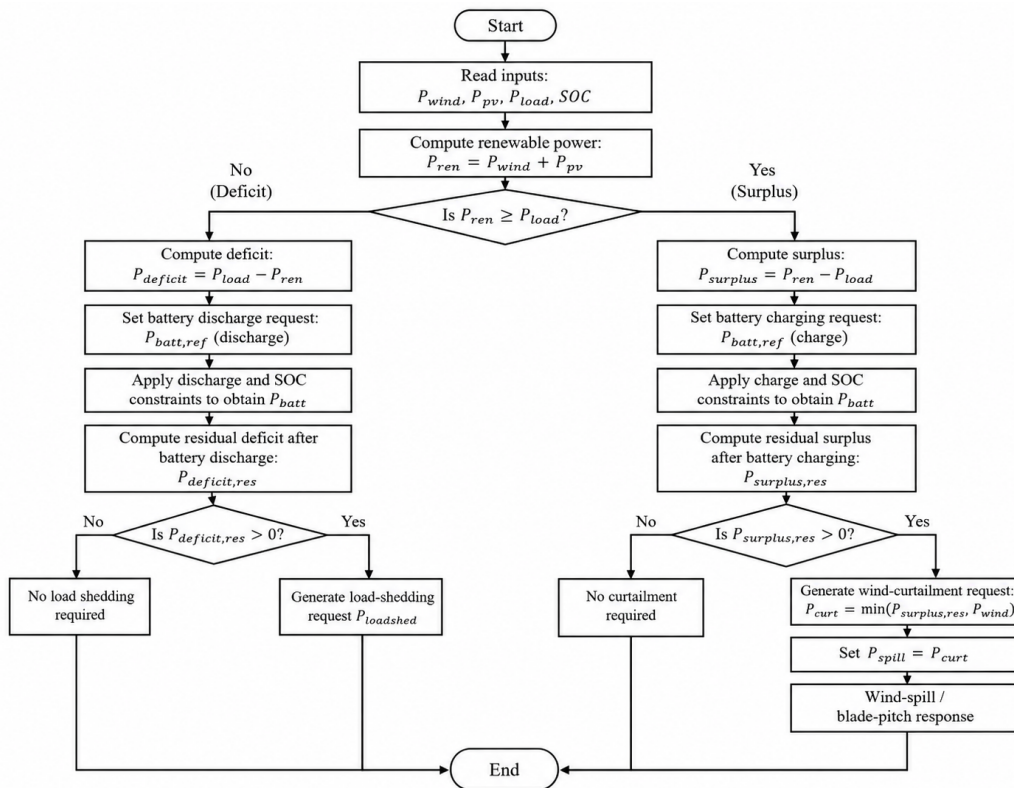


Figure 3.3: Flowchart of the supervisory EMS logic. Battery action is prioritised before residual surplus or residual deficit is assigned to curtailment or load shedding.

$P_{pv}$ , the load demand  $P_{load}$ , and the battery state of charge  $SOC$ . The EMS first calculates the aggregated renewable power,

$$P_{ren} = P_{wind} + P_{pv},$$

and compares it with the load demand.

If  $P_{ren} < P_{load}$ , the EMS enters the deficit branch. In this branch, the power deficit is calculated and a battery-discharge request is generated. The request is then limited by the implemented discharge-power and SOC constraints to obtain the feasible battery response  $P_{batt}$ . If a residual deficit remains after battery action, the EMS generates the load-shedding request  $P_{loadshed}$ . Otherwise, no load shedding is required.

If  $P_{ren} \geq P_{load}$ , the EMS enters the surplus branch. In this branch, the surplus power is calculated and a battery-charging request is generated. The request is limited by the implemented charge-power and SOC constraints to obtain the feasible battery response  $P_{batt}$ . If a residual surplus remains after battery charging, the EMS generates the wind-curtailment request  $P_{curt}$ . The curtailment request is then passed to the inherited wind-spill path through

$$P_{spill} = P_{curt},$$

so that the resulting wind-spill and blade-pitch response is handled by the inherited wind-turbine model. If no residual surplus remains, no curtailment is required.

The purpose of the flowchart is to show the control decisions and priority order of the EMS: battery action is applied first within its implemented constraints, residual surplus is assigned to wind curtailment, and residual deficit is assigned to load shedding.

The supervisory equations are defined in Chapter 2. They are not re-derived in this implementation chapter. The present chapter instead documents their Simulink realisation, the verified signal routing, and the simulation interfaces.

### 3.6 Implemented EMS Signal Structure

The internal EMS implementation contains the monitored signals required for examining the supervisory sequence. An enlarged functional view is used to show the principal signal routing without relying only on a dense unexpanded screenshot.

The EMS uses  $P_{wind}$  together with  $P_{pv}$  and  $P_{load}$  to establish the balancing request. The resulting battery reference is processed by the BESS branch. The EMS monitors both the initial imbalance and the remaining imbalance after battery action. This arrangement enables the Results chapter to distinguish:

- the original power condition before battery response;
- the feasible battery action under the implemented constraints;
- the residual quantity requiring curtailment or load shedding.

The sign convention is fixed throughout the implementation: positive  $P_{batt}$  denotes battery discharge, and negative  $P_{batt}$  denotes battery charging. This convention is applied consistently to  $P_{batt,ref}$ ,  $P_{batt}$ , the SOC evolution, and the interpretation of the simulation plots.

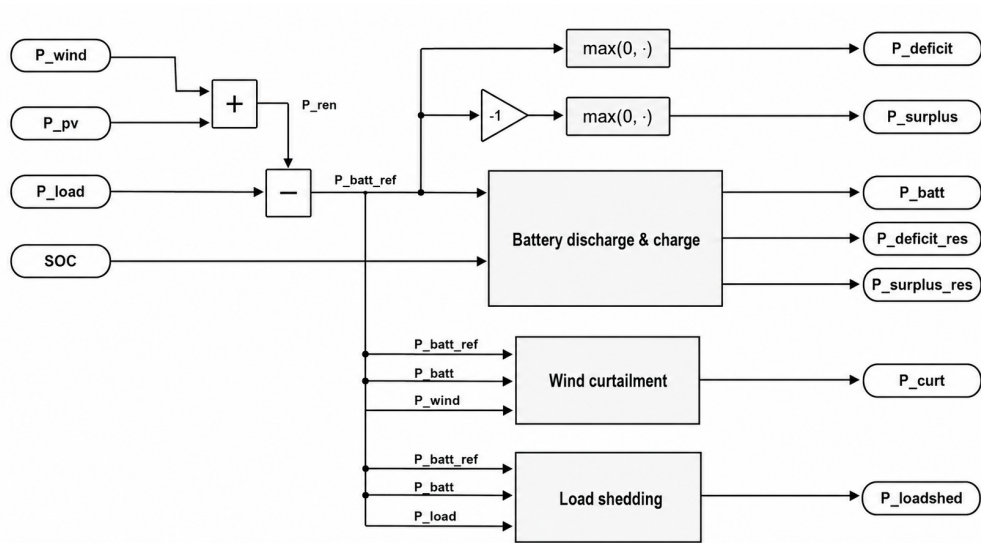


**Figure 3.4:** Enlarged functional view of the implemented EMS signal structure, including renewable aggregation, battery-reference formation, battery dispatch, residual mismatch, wind-curtailment request, and load-shedding request.

### 3.7 Battery Dispatch and BESS Interface

The battery dispatch logic is implemented as the preferred balancing action of the EMS. The requested battery power is processed through charge/discharge selection and constraint handling before a feasible battery response is supplied to the remainder of the supervisory model.

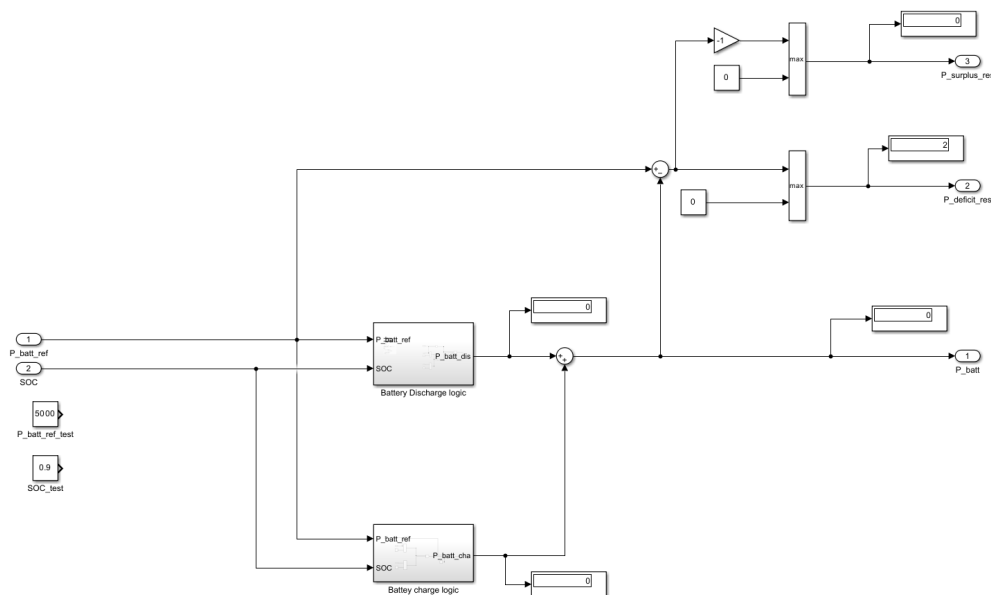


**Figure 3.5:** Implemented battery-dispatch subsystem used to produce the constrained battery-power response from the EMS battery reference and SOC condition.

The implemented dispatch structure contains two mutually exclusive operating branches. When the battery reference is positive, the discharge path is activated subject to the discharge-power and lower-SOC restrictions. When the battery reference is negative, the charging path is activated subject to the charging-power and upper-SOC restrictions.

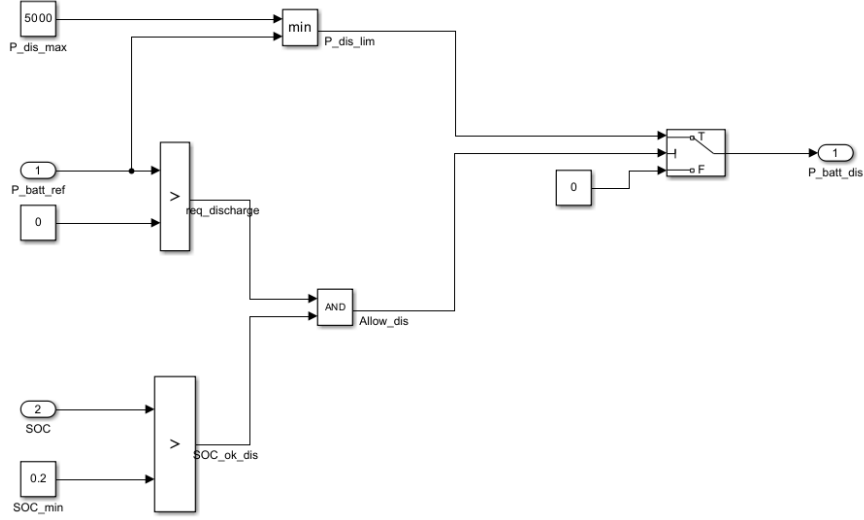


**Figure 3.6:** Implemented discharge branch of the BESS supervisory logic.

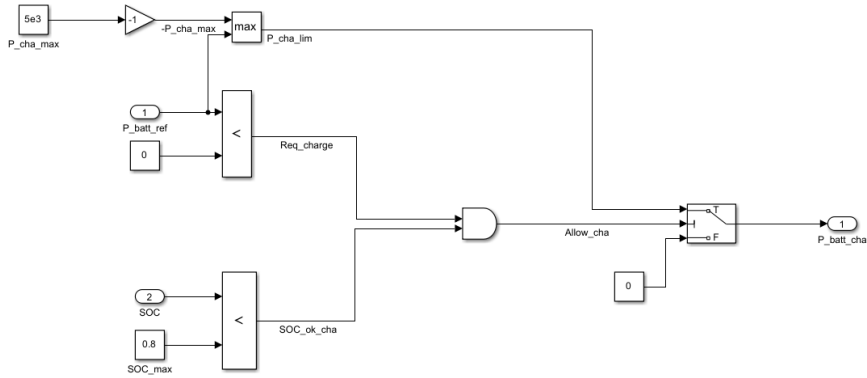


**Figure 3.7:** Implemented charge branch of the BESS supervisory logic.

The BESS interface is represented at supervisory level. It accepts the battery-power command, converts it to the current-direction convention used in the SOC integrator, and generates the simulated SOC trajectory. The implementation-specific conversion is

$$I_{\text{cmd}} = -\frac{P_{\text{batt}}}{V_{\text{nom}}}, \quad (3.2)$$

where the negative sign follows the current direction used in the implemented battery interface.

The principal EMS/BESS operating parameters are summarised in Table 3.1. The resulting SOC signal is a simulated output of the developed BESS interface. Although source and load profiles may originate from processed operating data, the

**Table 3.1:** Parameters of the implemented EMS/BESS supervisory operation.

Parameter	Symbol	Value	Interpretation
Nominal battery voltage	$V_{\text{nom}}$	400 V	Power-to-current interface voltage
Nominal charge capacity	$Q_{\text{nom}}$	12.5 Ah	Charge-capacity representation
Nominal stored energy	$E_{\text{nom}}$	5 kWh	Energy-storage representation
Initial state of charge	$SOC_0$	0.50	Initial SOC for the presented EMS/BESS simulation
Maximum charging-power magnitude	$P_{\text{ch,max}}$	5 kW	Charging appears as $-5$ kW under the adopted sign convention
Maximum discharging power	$P_{\text{dis,max}}$	5 kW	Positive discharge-power limit
Lower SOC threshold	$SOC_{\text{min}}$	0.20	Discharge-permission threshold
Upper SOC threshold	$SOC_{\text{max}}$	0.80	Charge-permission threshold

SOC trajectory evaluated in the Results chapter is generated by the implemented BESS response to the EMS battery-power command.

### 3.8 Residual Mismatch and Corrective-Action Paths

After the feasible battery response has been produced, the EMS evaluates whether any imbalance remains. The residual deficit and residual surplus signals connect battery feasibility to secondary corrective actions.

A residual deficit indicates that the requested discharge could not be fully delivered under the implemented BESS constraints. In that branch, the EMS issues a load-shedding request. A residual surplus indicates that renewable production remains above the quantity absorbed by the battery. In that branch, the EMS issues a wind-curtailment request.

The importance of these signals is methodological as well as numerical. They show whether a corrective action arises because of the initial source-load condition or because the BESS is unable to absorb or deliver the complete requested balancing power.

### 3.9 Implemented Wind-Curtailment Connection

The wind-curtailment path is the central connection between the developed EMS and the inherited wind-turbine model. The signal routing of the implemented

Simulink subsystem was checked during the revision. The three inputs of the implemented Wind Curtailment block are  $P_{\text{batt,ref}}$ ,  $P_{\text{batt}}$ , and  $P_{\text{wind}}$ . Consequently, the curtailment block implements the formulation given in Equation (2.15), in which the wind-side limiting signal is  $P_{\text{wind}}$ .

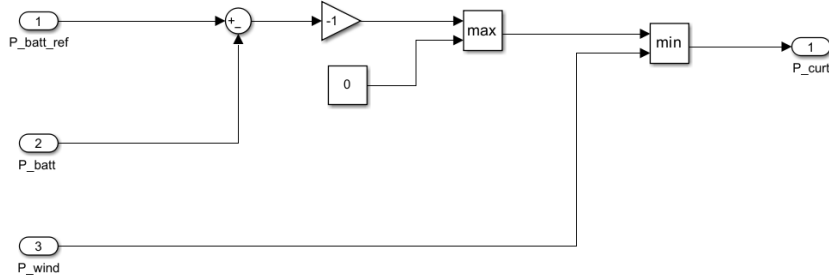


**Figure 3.8:** Implemented wind-curtailment subsystem. The third input to the minimum operation is the realised simulated wind-turbine output  $P_{\text{wind}}$ , consistent with the verified Simulink routing.

The generated EMS curtailment request is then connected to the inherited wind-spill input through

$$P_{\text{spill}} = P_{\text{curt}}. \quad (3.3)$$

This connection is essential for interpreting the short-term simulation. The EMS does not produce the final wind-power reduction by subtracting a curtailment value from the wind-power output after simulation. Instead, it sends a spilling-power request into the inherited turbine-control path. The wind-spill and blade-pitch dynamics then generate the resulting turbine response, consistent with the inherited Chalmers model description [17].

Accordingly, the short-term Results chapter evaluates not only the EMS request itself, but also the turbine-side consequence of that request through simulated blade-pitch response and realised wind-turbine output.

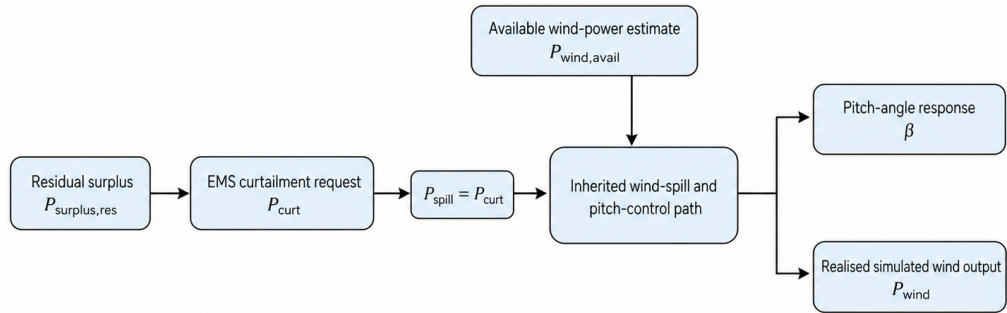
### 3.10 Implemented Load-Shedding Path

The load-shedding path represents the corrective action available when residual deficit remains after feasible battery discharge has been determined.

Within the supervisory hierarchy, load shedding is treated as a final corrective action after realised renewable generation and feasible battery support have been taken into account. The signal is monitored in the additional deficit-dominated Results case in order to show activation of the residual deficit branch.

### 3.11 System-Level Interface and Monitored Variables

The system-level interface organises the signals used for downstream power-balance interpretation. It is not used to establish a separate converter-level or three-phase



Flow of the wind-curtailment command from the EMS into the inherited wind-spill path.

**Figure 3.9:** Connection of the EMS curtailment output to the inherited wind-spill path. The request  $P_{\text{curt}}$  is passed as  $P_{\text{spill}}$ , after which the inherited turbine-control dynamics determine the realised wind-power response.

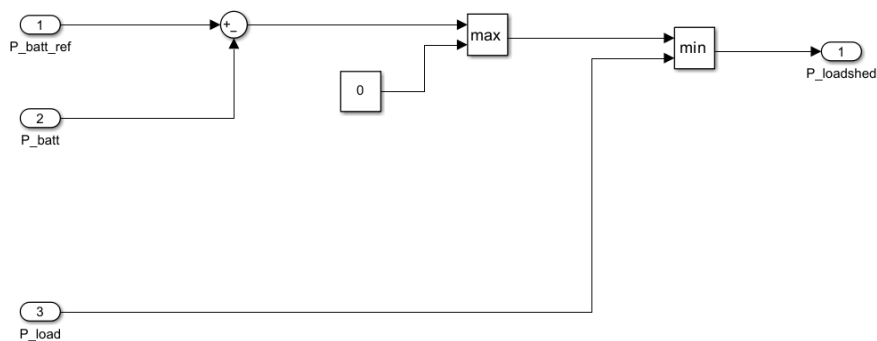


**Figure 3.10:** Implemented load-shedding subsystem driven by residual deficit after battery action.

active-power validation claim. Instead, it provides a consistent location for interpreting realised wind-turbine power, PV contribution, battery response, effective load condition, and remaining net-power behaviour at supervisory level.

To avoid double counting, the wind contribution used for downstream interpretation is the realised simulated wind-turbine output  $P_{\text{wind}}$ . When the EMS curtailment request has already been passed through the inherited wind-spill and blade-pitch path, its consequence is represented in  $P_{\text{wind}}$  itself and is not subtracted again as an additional algebraic correction.

The principal monitored variables are summarised in Table 3.2.

**Table 3.2:** Principal monitored variables in the implemented supervisory model.

Signal	Role in the implementation
$P_{\text{wind,avail}}$	Available wind-power estimate retained as a wind-side interpretation reference
$P_{\text{wind}}$	Realised simulated wind-turbine output used in renewable aggregation and as the wind-side input of the curtailment block
$P_{\text{pv}}$	Equivalent AC-side PV active-power contribution supplied to the EMS
$P_{\text{load}}$	Load-demand input supplied to the EMS
$P_{\text{batt,ref}}$	Battery-power request generated by the EMS
$P_{\text{batt}}$	Feasible battery-power response after power and SOC constraints
$SOC$	Simulated battery state of charge generated by the BESS interface
$P_{\text{deficit}}, P_{\text{surplus}}$	Initial mismatch components before feasible battery response
$P_{\text{deficit,res}}, P_{\text{surplus,res}}$	Residual mismatch components after battery action
$P_{\text{curt}}$	Wind-curtailment request generated from residual surplus
$P_{\text{spill}}$	Signal supplied to the inherited wind-spill input
$P_{\text{loadshed}}$	Load-shedding request generated from residual deficit

### 3.12 Long-Term EMS/BESS Simulation

The long-term simulation is used to examine operation of the developed EMS and BESS interface over a time-varying operating interval. In this simulation, the source and load profiles serve as input conditions to the supervisory model. The principal purpose is to determine how the EMS generates battery charging commands, how the implemented BESS produces an SOC trajectory, and how residual surplus or

deficit is converted into corrective-action requests.

The long-term simulation evaluates the following generated outputs:

- battery reference  $P_{\text{batt,ref}}$ ;
- constrained battery response  $P_{\text{batt}}$ ;
- simulated *SOC* trajectory;
- original deficit and surplus signals;
- residual deficit and surplus after battery action;
- wind-curtailment and load-shedding requests.

This simulation is an EMS/BESS evaluation rather than a turbine blade-pitch-response study. Turbine-side pitch dynamics are evaluated separately in the short-term integrated simulation, where the EMS curtailment output is explicitly connected to the inherited wind-spill path.

### 3.13 Short-Term Integrated EMS–Wind-Turbine Simulation

The short-term simulation evaluates interaction between the developed EMS and the inherited wind-turbine model. The integrated model is simulated continuously over the interval from 0 s to 120 s. The complete interval is retained because the inherited wind-turbine subsystem includes start-up and dynamic-state behaviour that influences the subsequent realised power and blade-pitch response.

The principal quantities examined in this simulation are:

- measured and estimated wind-speed signals used to characterise the wind-side operating condition;
- $P_{\text{wind,avail}}$ , retained as an available wind-power interpretation reference;
- $P_{\text{wind}}$ , the realised wind-turbine output used in the EMS and in the implemented curtailment block;
- $P_{\text{curt}}$  and  $P_{\text{spill}}$ , which document the EMS request and its connection to the wind-spill path;
- simulated blade-pitch response and realised simulated wind-turbine power.

This arrangement allows the short-term results to demonstrate the curtailment interaction: residual surplus generates an EMS command, the command is passed to the inherited wind-spill input, and the inherited turbine model produces an associated blade-pitch and realised-power response.

### 3.14 Traceability from Theory to Implementation

The theory chapter defines the supervisory power-balance quantities and the logic of battery prioritisation, residual mismatch, curtailment, and load shedding. The present chapter maps those quantities to executable Simulink signals.

The implementation traceability is as follows:

- $P_{\text{wind}}$ ,  $P_{\text{pv}}$ , and  $P_{\text{load}}$  are the active-power quantities used to evaluate the balancing condition;

- $P_{\text{wind,avail}}$  is retained as an available wind-power interpretation reference, not as the implemented curtailment-block input;
- $P_{\text{batt,ref}}$  is generated by the EMS and passed to the BESS branch;
- $P_{\text{batt}}$  and  $SOC$  are generated by the implemented BESS response;
- $P_{\text{deficit,res}}$  and  $P_{\text{surplus,res}}$  identify the remaining balancing requirement after battery action;
- the Wind Curtailment subsystem implements Equation (2.15) using  $P_{\text{wind}}$  as its wind-side limiting input;
- $P_{\text{curt}}$  is connected to the inherited wind-spill input as  $P_{\text{spill}}$ ;
- $P_{\text{loadshed}}$  represents the corrective action associated with residual deficit;
- $P_{\text{wind}}$  is the realised wind-turbine output used for downstream power-balance interpretation after turbine-side curtailment response.

### 3.15 Implementation Scope

The implemented model gives an executable supervisory-control framework for islanded operation with wind generation, PV generation, battery storage, and load demand. The EMS chain, the BESS interface, residual-mismatch processing, wind-curtailment request, load-shedding request, and the connection from EMS to the wind-spill input are all included in the simulation structure.

The two simulation groups are used for different but related purposes. The long-term EMS/BESS simulation shows how time-varying operating inputs are changed into battery operation, SOC evolution, residual imbalance, and corrective-action requests. The short-term integrated EMS-wind-turbine simulation shows how the curtailment request goes through the inherited wind-spill and blade-pitch structure, and then produces a dynamic response on the turbine side.

Based on this, the implemented model gives a usable basis for evaluating the supervisory active-power coordination developed in this thesis, as well as its interaction with the inherited wind-turbine subsystem.



# 4

## Results and Discussion

### 4.1 Overview of the Result Analysis

This chapter evaluates the behaviour of the developed supervisory Energy Management System (EMS), the simplified BESS interface, and their interaction with the inherited wind-turbine model under islanded operating conditions. The analysis is divided into three related parts, so that the different result types can be discussed more clearly.

The first part is the long-term EMS/BESS simulation. In this case, measurement-derived profiles of available wind power, photovoltaic power, and load demand are used as replay input conditions; these profiles describe the operating condition of the islanded system. The main outputs are then produced by the implemented EMS and BESS interface, including the battery power reference, constrained battery power, simulated SOC, original deficit and surplus, residual mismatch, curtailment request, and load-shedding request. This part is used to check the supervisory energy-management behaviour over a longer operating period.

The second part is an additional EMS-level deficit validation case. In this case, a prescribed stepwise load-demand profile is applied through the Signal Editor, so that there is an interval where the load is higher than the combined renewable contribution and the available battery discharge capability. This case is used to check the deficit-handling branch and the load-shedding branch of the EMS.

The third part is a 0–120 s EMS and wind-turbine interaction case. In this case, prescribed equivalent AC-side photovoltaic-power and load-demand profiles are supplied to the EMS, while the wind-power contribution comes from the dynamic wind-turbine simulation. The complete interval is kept, because the start-up history and the internal dynamic-state development of the inherited wind-turbine model should not be removed. This short-term case is used to examine how the EMS curtailment request is sent to the wind-spill input, and how it is shown through the simulated blade-pitch response and wind-power response.

This separation is useful for interpreting the results. The long-term case mainly evaluates energy-management behaviour and SOC evolution; the additional deficit case checks the load-shedding branch; the short-term case focuses on the wind-spill and pitch-related turbine response. In this way, the measurement-derived input profiles, the EMS/BESS simulation outputs, and the wind-turbine model responses are kept separated in the discussion.

The organisation of the result analysis follows the layered EMS interpretation used in microgrid energy-management studies, where supervisory dispatch, storage-state

constraints, and lower-level component responses are related to each other, but they are still treated as different layers [3, 8, 7].

## 4.2 Classification of Result Signals

Before presenting the results, the main signals are classified according to their role in the simulation. This distinction is necessary because the result chapter uses both measurement-derived input profiles and outputs generated by the implemented EMS, BESS interface, and inherited wind-turbine model.

**Table 4.1:** Classification of signals used in the result analysis.

Signal group	Examples	Interpretation
Replay input profiles	$P_{\text{wind,avail}}$ , $P_{\text{pv}}$ , $P_{\text{load}}$	Applied source and demand operating conditions.
EMS/BESS outputs	$P_{\text{batt}}$ , SOC, $P_{\text{curt}}$ , $P_{\text{loadshed}}$	Supervisory balancing responses generated by the model.
Wind-turbine reference signals	Measured/reference power and blade pitch	Normal-operation context for the inherited turbine data.
Wind-turbine simulated outputs	$P_{\text{wind}}$ , simulated blade pitch	Response under the EMS-supplied wind-spill command.

The classification in Table 4.1 is used throughout the chapter. In particular, the long-term EMS/BESS results and the additional deficit validation case are not interpreted as direct measurements. They are simulation outputs produced by the implemented EMS and BESS interface under prescribed or measurement-derived operating profiles. The short-term wind-turbine results, in contrast, include both measured/reference signals and simulated wind-model responses, and these are discussed separately.

## 4.3 Simulation Parameters Used in the Result Cases

Table 4.2 summarises the main simulation parameters and operating settings used for the result cases. The values are included to make the result interpretation traceable and to clarify the modelling scale of the EMS/BESS and wind-turbine simulations. Positive battery power denotes discharge to the islanded system, whereas negative battery power denotes charging. Therefore, the charging-power magnitude  $P_{\text{ch,max}} = 5$  kW appears in the battery-power signal as a lower charging limit of  $-5$  kW. The photovoltaic contribution is interpreted as an equivalent AC-side active-power input at the EMS power-balance interface, while load demand is represented as an active-power input. In the additional validation case, a stepwise load profile is applied to activate the deficit-handling branch.

**Table 4.2:** Parameters used in the result simulations.

<b>Parameter</b>	<b>Symbol</b>	<b>Value</b>	<b>Unit</b>
Long-term simulation horizon	$T_{\text{long}}$	1800	s
Long-term fixed step size	$\Delta t_{\text{long}}$	0.05	s
Short-term simulation horizon	$T_{\text{short}}$	120	s
Short-term fixed step size	$\Delta t_{\text{short}}$	$5 \times 10^{-5}$	s
Battery nominal voltage	$V_{\text{batt}}$	400	V
Battery nominal capacity	$C_{\text{batt}}$	12.5	Ah
Battery nominal energy	$E_{\text{batt}}$	5	kWh
Maximum charging-power magnitude	$P_{\text{ch,max}}$	5	kW
Maximum discharging power	$P_{\text{dis,max}}$	+5	kW
Lower SOC threshold	$\text{SOC}_{\text{min}}$	0.20	–
Upper SOC threshold	$\text{SOC}_{\text{max}}$	0.80	–
Wind-turbine rated-power cap	$P_{\text{wind,rated}}$	25	kW
Minimum blade-pitch angle	$\beta_{\text{min}}$	0.0349	rad
Maximum blade-pitch rate	$\dot{\beta}_{\text{max}}$	0.2	rad/s

The parameter table is used as a reference for the following result interpretation. In particular, the approximately 5 kW charging and discharging limits explain why residual surplus or residual deficit can remain after the battery has responded.

## 4.4 Long-Term EMS/BESS Simulation

### 4.4.1 Long-Term Source and Load Profiles

The long-term case uses measurement-derived source and load profiles as replay inputs to the EMS-level simulation. These profiles define the external operating condition of the islanded system. The EMS and BESS interface then process these input profiles and generate the corresponding supervisory outputs.

Figure 4.1 shows the available wind power, photovoltaic power, and load demand used in the long-term simulation.

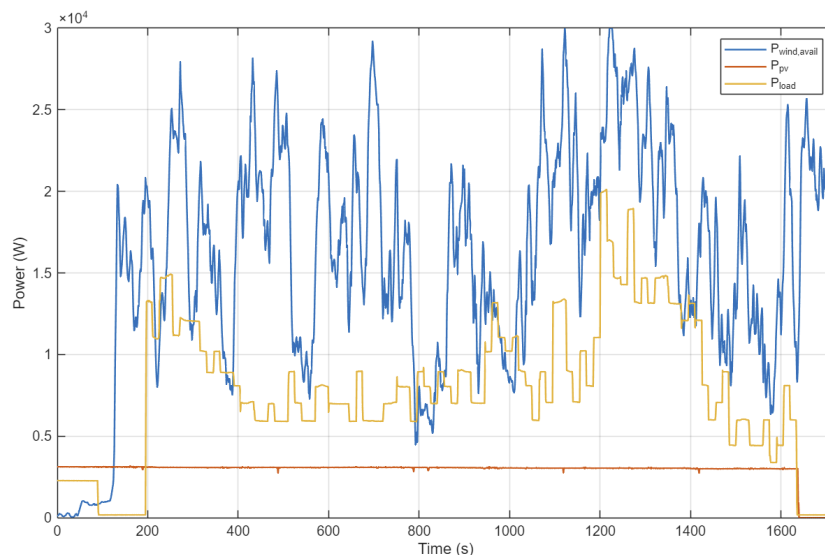


**Figure 4.1:** Long-term source and load profiles used as replay inputs for the EMS/BESS simulation.

The profiles in Figure 4.1 define the operating condition for the long-term EMS/BESS replay. The battery-power response, SOC evolution, residual mismatch, curtailment request, and load-shedding request are not prescribed in this figure. They are generated by the implemented EMS/BESS model and are analysed in the following figures.

The available wind-power profile is the dominant renewable input in this case. The photovoltaic contribution remains comparatively small, while the load demand varies over the simulation horizon. The resulting operating condition is mainly surplus dominated. Therefore, the expected EMS response is to request battery charging first and then activate curtailment when the BESS cannot absorb the full renewable surplus.

### 4.4.2 Battery Reference and Constrained Battery Power

Figure 4.2 shows the long-term battery reference and the constrained battery power generated by the EMS/BESS simulation.

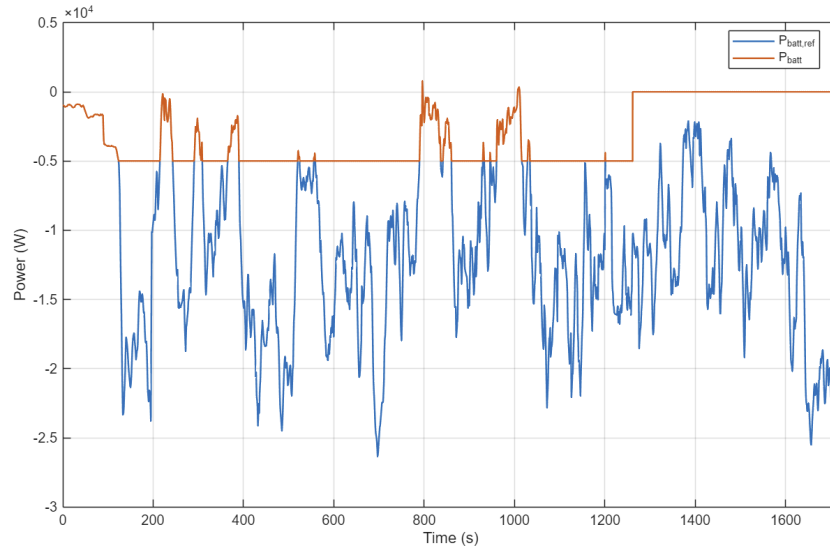


**Figure 4.2:** Battery reference and constrained battery power in the long-term case.

The battery reference  $P_{\text{batt,ref}}$  is mostly negative, indicating that the EMS requests battery charging during the surplus-dominated operating condition. The constrained battery power  $P_{\text{batt}}$  follows the direction of the reference when charging is allowed, but it is limited by the BESS constraints. When the feasible charging action is restricted, the remaining power imbalance is passed to the residual-mismatch calculation.

This result verifies the first stage of the EMS hierarchy. The EMS initially assigns the renewable-load mismatch to the battery. The BESS interface then applies the power and SOC constraints before any secondary corrective action is activated.

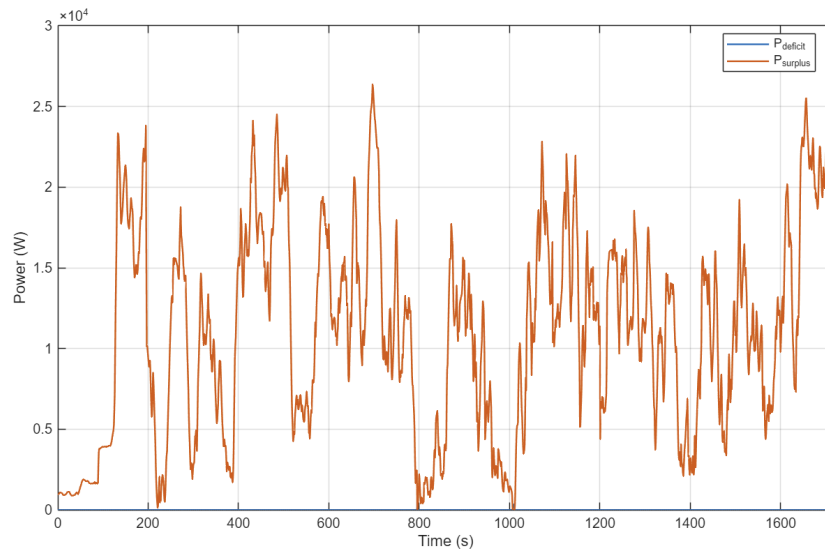
### 4.4.3 Original Deficit and Surplus

Figure 4.3 shows the original deficit and surplus computed by the EMS before constrained battery action.

The deficit signal remains close to zero for most of the simulation, while the surplus signal is frequently positive. This confirms that the long-term operating condition is mainly characterised by excess renewable generation. The EMS therefore operates primarily in surplus-handling mode: the battery is used as the first balancing unit, and remaining surplus is transferred to the curtailment branch.

### 4.4.4 Simulated SOC Evolution

Figure 4.4 shows the simulated SOC response obtained from the BESS interface. The SOC increases from approximately 0.50 to the selected upper operating limit. This behaviour is consistent with the negative battery power shown in Figure 4.2.



**Figure 4.3:** Original deficit and surplus in the long-term case.

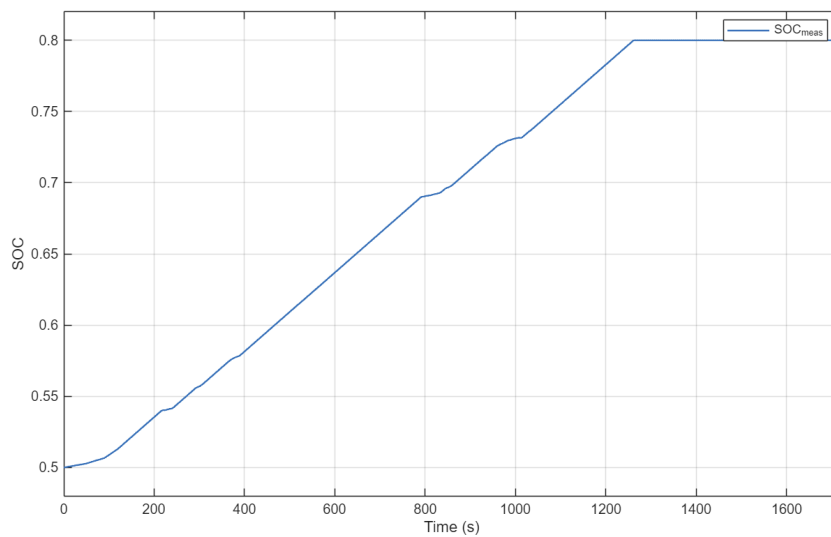


**Figure 4.4:** Simulated battery SOC in the long-term case.

The battery absorbs surplus energy over the long-term horizon until further charging is restricted by the upper SOC limit. After this point, the EMS cannot rely on the battery alone to absorb the remaining surplus.

This result is important because it shows that SOC is a state produced by the BESS response in the long-term simulation. The SOC trajectory is therefore part of the simulated EMS/BESS behaviour, not merely a static plotting signal.

#### 4.4.5 Residual Mismatch After Battery Action

Figure 4.5 shows the residual deficit and residual surplus after constrained battery action.

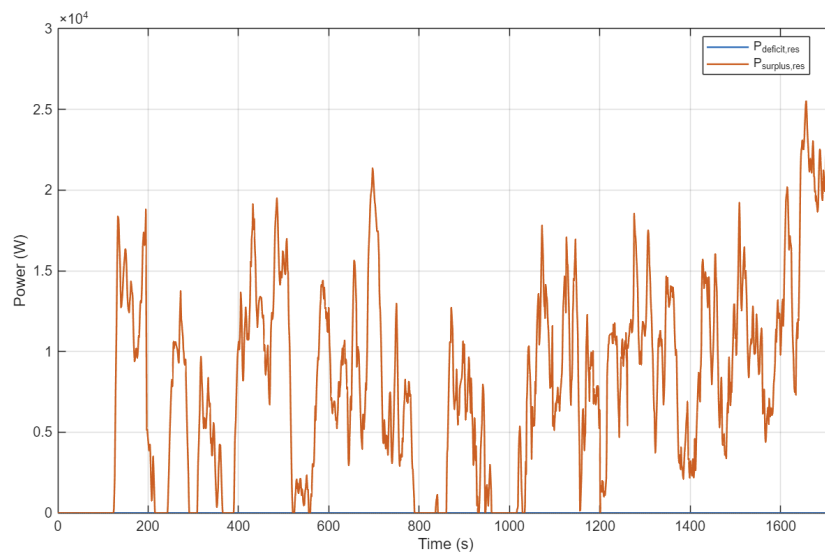


**Figure 4.5:** Residual mismatch after battery action in the long-term case.

The residual deficit remains close to zero, meaning that the long-term case does not require sustained load shedding. In contrast, the residual surplus is positive over significant parts of the simulation. This residual surplus appears when the requested charging action exceeds what the constrained BESS response can provide.

The residual-mismatch result provides the link between battery dispatch and secondary corrective action. The EMS does not immediately curtail wind power. It first uses the battery as the preferred balancing mechanism. Curtailment is activated only for the surplus that remains after constrained battery action.

#### 4.4.6 Curtailment and Load-Shedding Requests

Figure 4.6 shows the corrective-action signals generated by the EMS.

The curtailment request follows the residual surplus. This verifies the surplus-handling logic of the EMS: after the battery reaches its feasible charging response, the remaining surplus is converted into a wind-curtailment request. The load-shedding signal remains zero because the residual deficit is approximately zero in this long-term case.

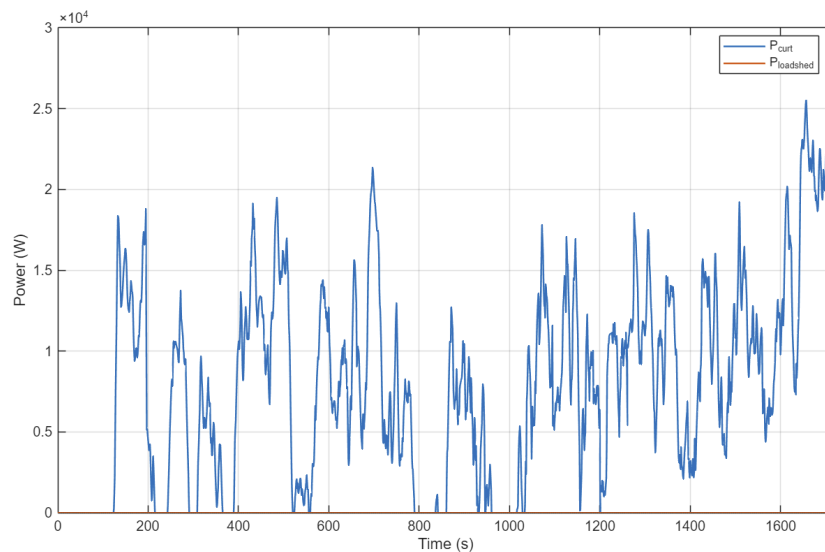


**Figure 4.6:** Curtailment and load-shedding requests in the long-term case.

Taken together, the long-term results show that the measurement-derived input profiles are converted by the implemented EMS/BESS model into coherent simulated supervisory outputs. The model generates a charging reference, applies BESS constraints, produces SOC evolution, identifies residual surplus, and converts that residual surplus into a curtailment request.

## 4.5 Additional Deficit and Load-Shedding Validation Case

### 4.5.1 Purpose of the Additional Validation Case

The long-term case presented above is mainly surplus dominated. It therefore verifies the sequence from renewable surplus to battery charging and then to wind-power curtailment. To also verify the opposite EMS branch, an additional EMS-level validation case is introduced in this section.

In this case, the load-demand profile is prescribed through the Signal Editor so that a selected interval contains a load demand higher than the available renewable contribution and higher than the discharge support that can be provided by the battery. The purpose is not to create a new wind-turbine dynamic study, but to verify the deficit-side EMS branch. In this branch, the detected initial deficit first produces a permissible battery-discharge response; any remaining residual deficit then produces the load-shedding request. This sequence is the deficit-side counterpart of the surplus-side curtailment logic.

### 4.5.2 Prescribed Load Profile

Figure 4.7 shows the prescribed load-demand profile used in the deficit validation case.

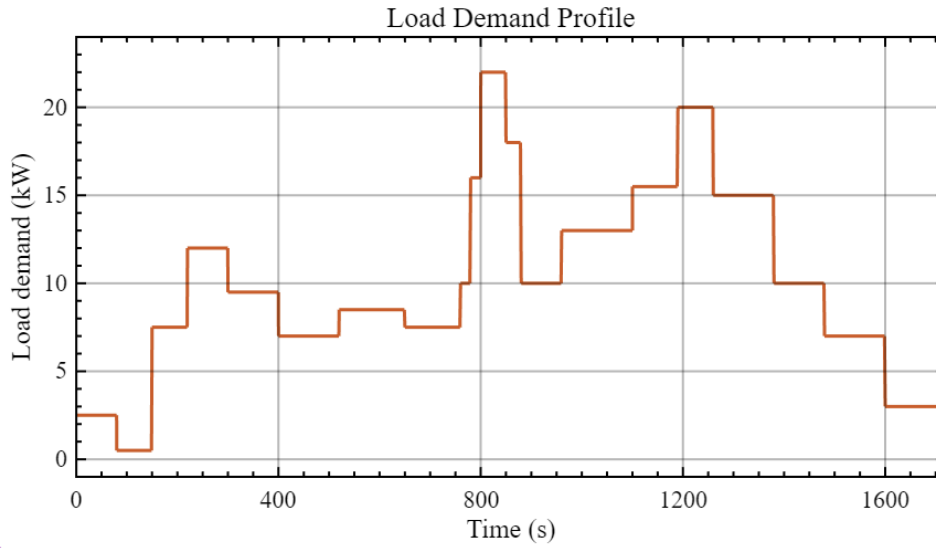


**Figure 4.7:** Prescribed load profile in the deficit-validation case.

The load profile is made stepwise on purpose, because this makes the EMS response easier to read. When the load changes, the change in the deficit signal can be compared with it more directly. The main interval is around 800–860 s; during this time, the load demand rises to about 22 kW. This interval is used to test whether the EMS can send the remaining deficit to the load-shedding branch after the battery discharge limit has already been reached.

### 4.5.3 Original Power Deficit

Figure 4.8 shows the original power deficit computed by the EMS before constrained battery action.

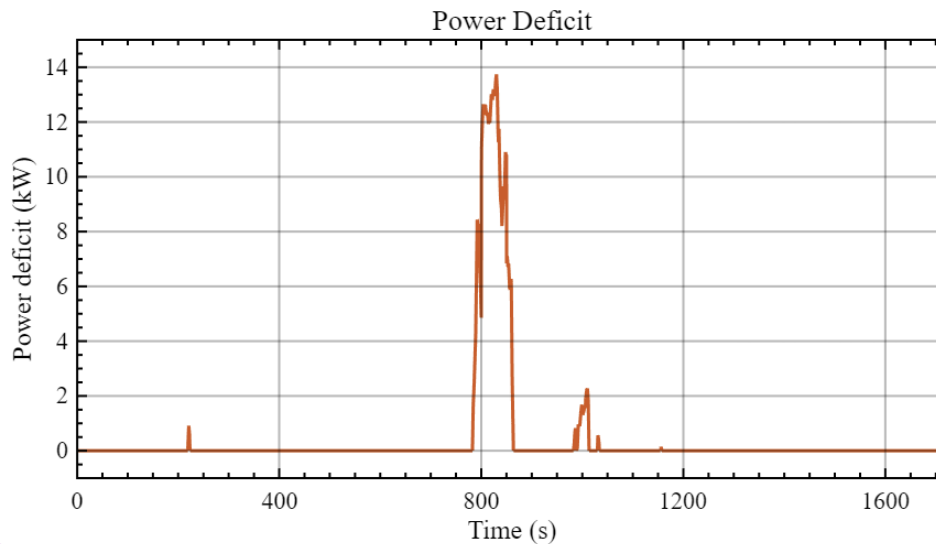


**Figure 4.8:** Original power deficit  $P_{\text{deficit}}$  in the additional deficit validation case.

The original deficit is close to zero over most of the simulation horizon, but a clear deficit appears around 800–860 s. The peak deficit is approximately 13–14 kW.

This verifies that the prescribed load profile successfully creates a deficit-dominated operating interval. A smaller deficit also appears around 1000 s, but this smaller imbalance is mostly within the battery discharge capability and therefore does not lead to sustained load shedding.

#### 4.5.4 Battery Response in the Deficit Case

Figure 4.9 shows the constrained battery power during the additional validation case.

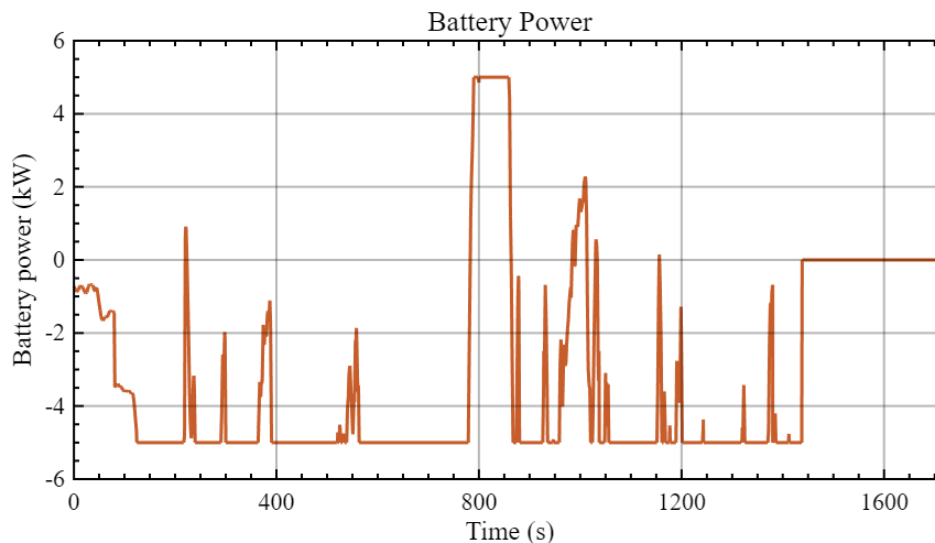


**Figure 4.9:** Constrained battery power  $P_{\text{batt}}$  in the additional deficit validation case. Positive power corresponds to battery discharge and negative power corresponds to battery charging.

During the main deficit interval around 800–860 s, the battery discharges at approximately 5 kW. This is consistent with the discharge limit used in the BESS interface. The battery therefore provides the first corrective action, but it does not fully remove the original deficit. This behaviour is expected from the EMS hierarchy: the battery is used before load shedding, but it is not treated as an unlimited power source.

#### 4.5.5 Simulated SOC in the Deficit Case

Figure 4.10 shows the simulated battery SOC during the additional deficit validation case.

The SOC trajectory provides the state-based interpretation of the battery response shown in Figure 4.9. Although the overall validation case still includes charging intervals before and after the imposed high-load period, a local SOC decrease is observed around 800–860 s. This interval corresponds to the main deficit condition, during which the battery discharges at approximately 5 kW to support the load.

The local SOC decrease confirms that the battery is used as the first corrective action in the deficit branch. After the discharge-power limit is reached, the remaining mismatch appears as residual deficit and is subsequently converted into the

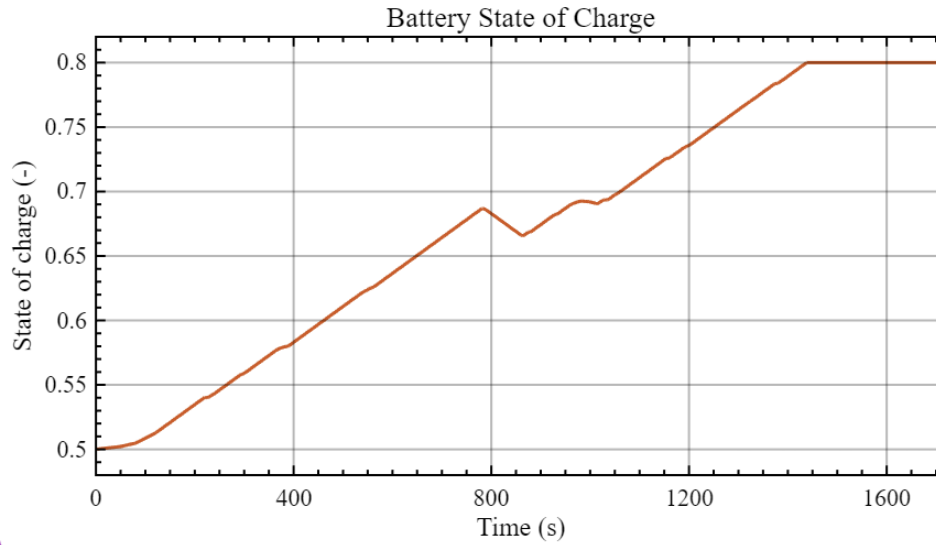


**Figure 4.10:** Simulated battery SOC in the additional deficit validation case.

load-shedding request. The SOC result therefore complements the battery-power, residual-deficit, and load-shedding plots by showing the corresponding battery-state response.

#### 4.5.6 Residual Deficit After Battery Dispatch

Figure 4.11 shows the residual deficit after the constrained battery response.

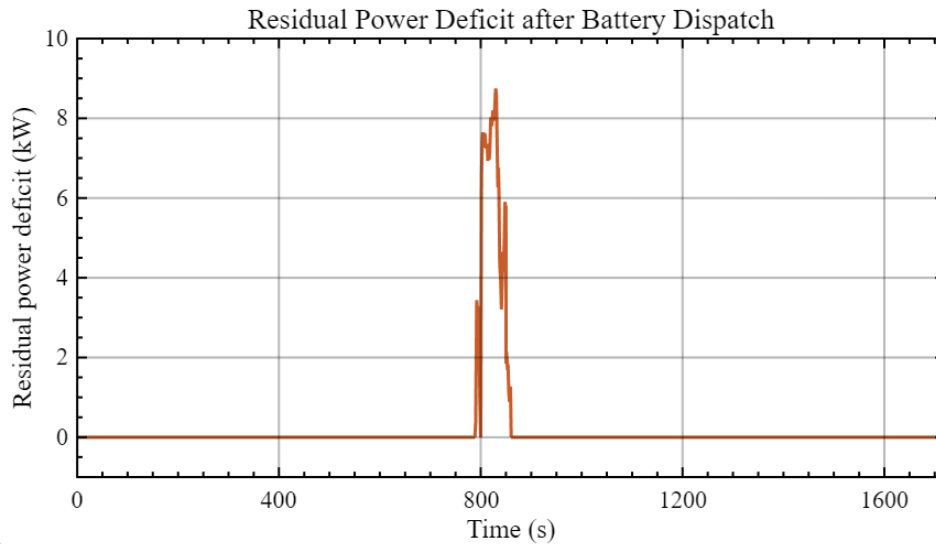


**Figure 4.11:** Residual power deficit  $P_{\text{deficit,res}}$  after constrained battery action in the additional deficit validation case.

The residual deficit appears during the same interval as the main original deficit. Its peak is approximately 8–9 kW, which is consistent with an original deficit of approximately 13–14 kW and a battery discharge response of approximately 5 kW. This result confirms that the EMS does not send the entire original deficit directly to load shedding. Instead, the battery contribution is applied first, and only the

unresolved part remains as  $P_{\text{deficit,res}}$ .

### 4.5.7 Load-Shedding Response

Figure 4.12 shows the load-shedding request generated by the EMS.

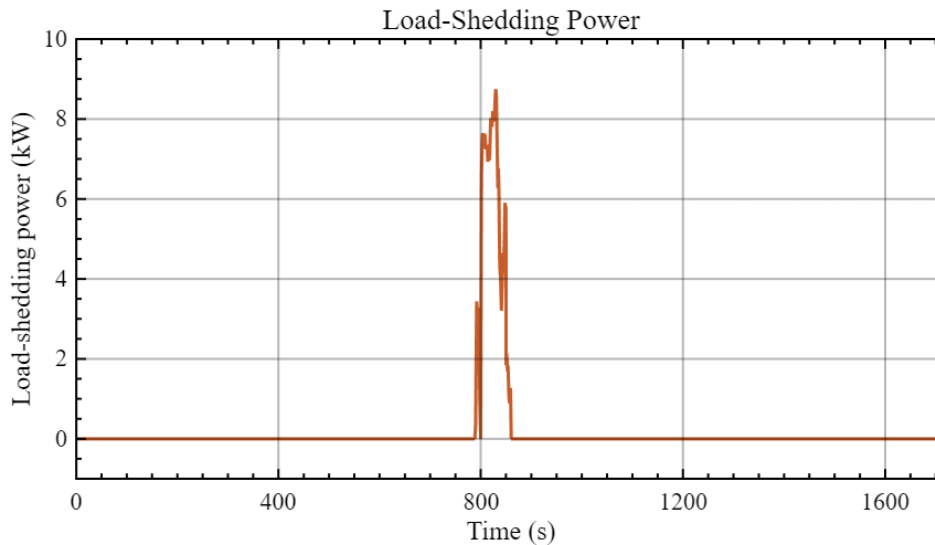


**Figure 4.12:** Load-shedding request  $P_{\text{loadshed}}$  generated in the additional deficit validation case.

The load-shedding request follows the residual-deficit signal during the main deficit interval. Its peak value is approximately 8–9 kW, which agrees with the residual deficit shown in Figure 4.11. Outside the deficit interval,  $P_{\text{loadshed}}$  returns to zero. This case verifies the deficit-handling branch of the EMS. When the load exceeds the renewable contribution and the battery discharge limit, the EMS first uses the battery, calculates the remaining deficit, and then activates load shedding for the unresolved part. Together with the surplus-dominated long-term case, the additional validation case demonstrates both corrective branches of the EMS: curtailment under residual surplus and load shedding under residual deficit.

## 4.6 Short-Term EMS and Wind-Turbine Interaction

### 4.6.1 Purpose and Operating Inputs of the Short-Term Case

The short-term case examines the interaction between the EMS, BESS interface, and dynamic wind-turbine model over the complete interval from 0 s to 120 s. The complete interval is retained in order to preserve the wind-turbine start-up history and the internal dynamic-state evolution before the subsequent surplus-handling response is analysed. In this simulation, the photovoltaic-power and load-demand profiles are supplied as prescribed operating inputs to the EMS, where the photovoltaic quantity is interpreted as an equivalent AC-side active-power contribution,

while the realised wind-power contribution is provided by the dynamic wind-turbine model.

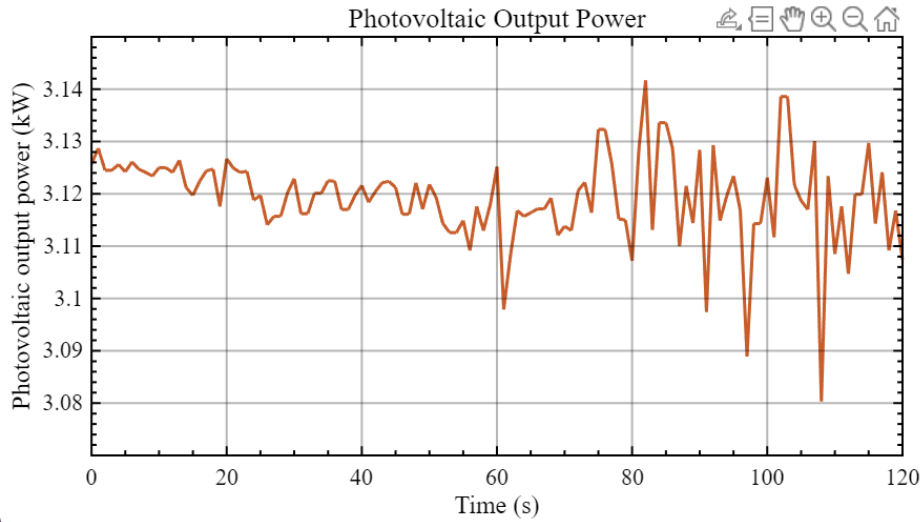


**Figure 4.13:** Equivalent AC-side photovoltaic active-power input  $P_{pv}$  in the short-term EMS simulation.

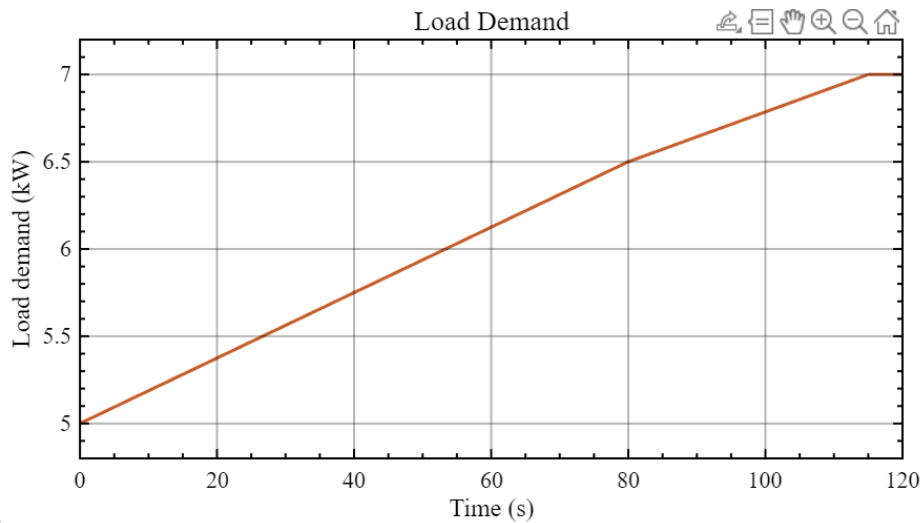


**Figure 4.14:** Prescribed load demand  $P_{load}$  used as an EMS operating input in the 0–120 s short-term simulation.

Figures 4.13 and 4.14 identify the prescribed photovoltaic-power and load-demand conditions used by the EMS together with the dynamically simulated wind-turbine power. The photovoltaic power remains approximately constant around 3.1 kW, while the load demand increases from approximately 5 kW to 7 kW during the interval. Before the wind-turbine output becomes available, the photovoltaic contribution alone is lower than the load demand, which is consistent with the initial power deficit and battery-discharge request shown later in this section. Once the simulated wind-turbine output is established, the total renewable production exceeds the load demand and the EMS changes from deficit handling to surplus handling.

The central interface relation in the short-term case is

$$P_{\text{spill}} = P_{\text{curt}}, \quad (4.1)$$

where the curtailment request generated from residual surplus is supplied as the wind-spill command to the turbine-control path. The short-term result analysis therefore follows the implemented signal-flow order described in Chapter 3: the original deficit or surplus determines the battery action; any residual surplus generates  $P_{\text{curt}}$ ; and the direct assignment  $P_{\text{spill}} = P_{\text{curt}}$  allows the blade-pitch and realised wind-power responses of the inherited turbine model to be examined.

### 4.6.2 Wind-Side Operating Condition and Turbine Start-Up Response

Figure 4.15 shows the measured wind-speed condition over the complete short-term interval.

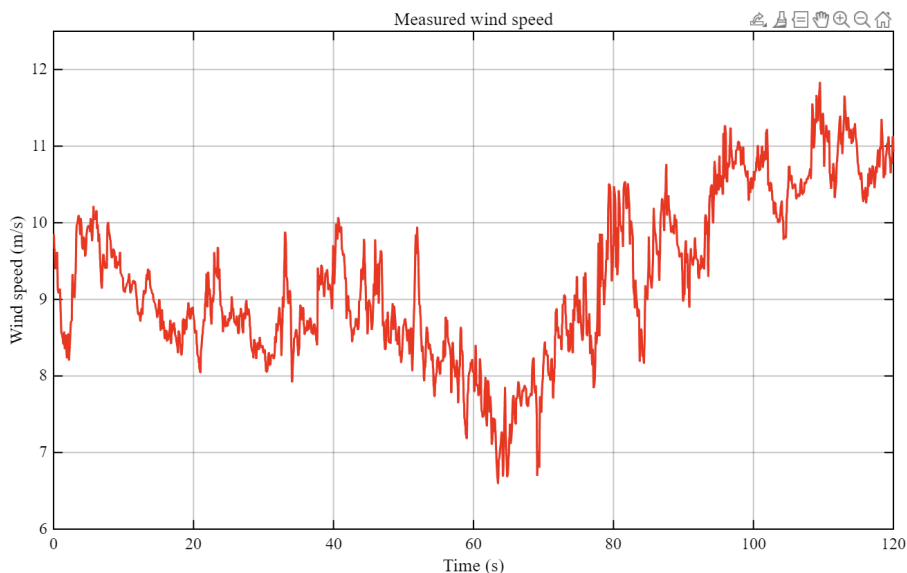


**Figure 4.15:** Measured wind-speed condition in the short-term simulation.

The measured wind speed varies within approximately 6.5–12 m/s over the presented interval. In particular, a non-zero external wind condition is already present during the initial portion of the simulation. The absence of simulated wind-turbine output power during the initial interval is therefore not interpreted as an absence of measured wind.

Figure 4.16 shows the estimated wind-speed signal generated internally in the wind-turbine modelling path.

The estimated wind-speed signal is initially close to its lower value and subsequently increases as the turbine-side simulated operating state develops. It reaches a comparatively stable range of approximately 10–11 m/s during the later part of the interval. The difference between the measured and estimated wind-speed signals is consistent with their different roles: the former is the external wind-side condition, whereas the latter is an internal model quantity associated with the turbine-side operating state.

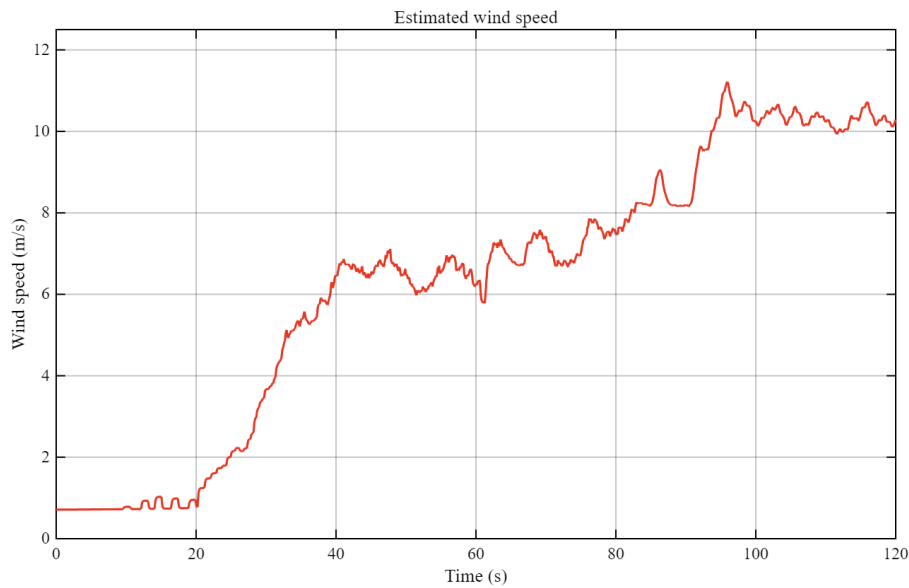


**Figure 4.16:** Estimated wind-speed signal in the wind-turbine model.

Figure 4.17 shows the corresponding available wind-power estimate.

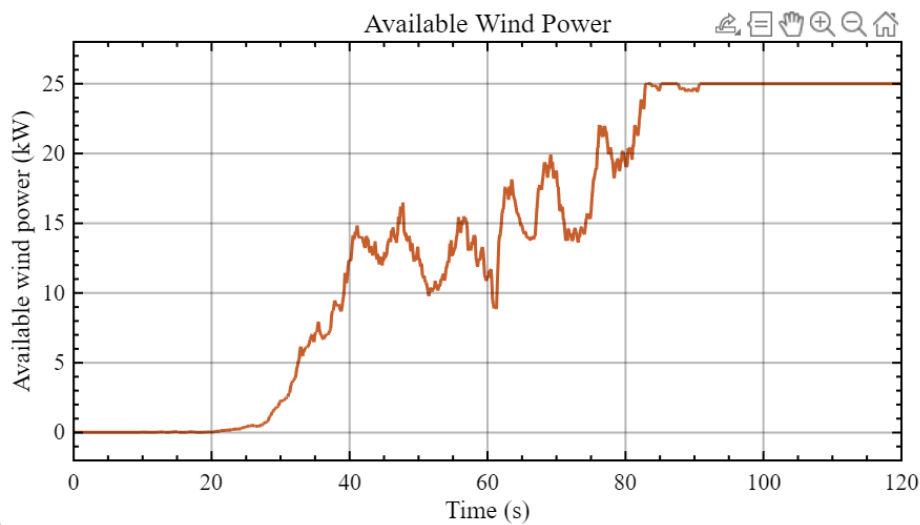


**Figure 4.17:** Available wind-power estimate  $P_{\text{wind,avail}}$  generated by the wind-turbine model during the 0–120 s short-term simulation.

The available wind-power estimate is initially close to zero and increases as the turbine-side estimated operating condition becomes established. After approximately 84 s, it reaches the rated-power cap of approximately 25 kW. This signal provides the wind-side availability reference against which the realised simulated wind-turbine power and the requested wind-power curtailment are interpreted.

Figure 4.18 presents the realised simulated wind-turbine output power.

The realised simulated wind-turbine output remains zero during the initial start-up interval and begins to increase at approximately  $t = 53$  s. It then passes through a transient power-producing region before settling at approximately 16.5–17 kW after approximately 84 s. Since the full interval is simulated continuously from  $t = 0$  s,

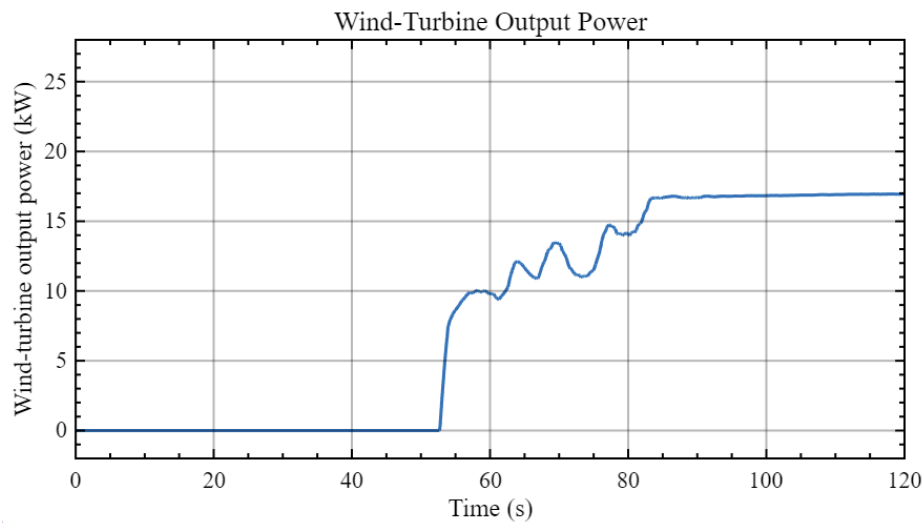


**Figure 4.18:** Realised simulated wind-turbine output power  $P_{\text{wind}}$  during the 0–120 s short-term simulation.

the initial zero-power period is interpreted as part of the wind-turbine start-up and internal state-establishment response, rather than as zero wind availability or as an EMS curtailment action.

### 4.6.3 Reference and Simulated Wind-Turbine Power

Figure 4.19 compares the normal-operation measured/reference wind-turbine power with the realised simulated wind-turbine power under the EMS-supplied wind-spill command.

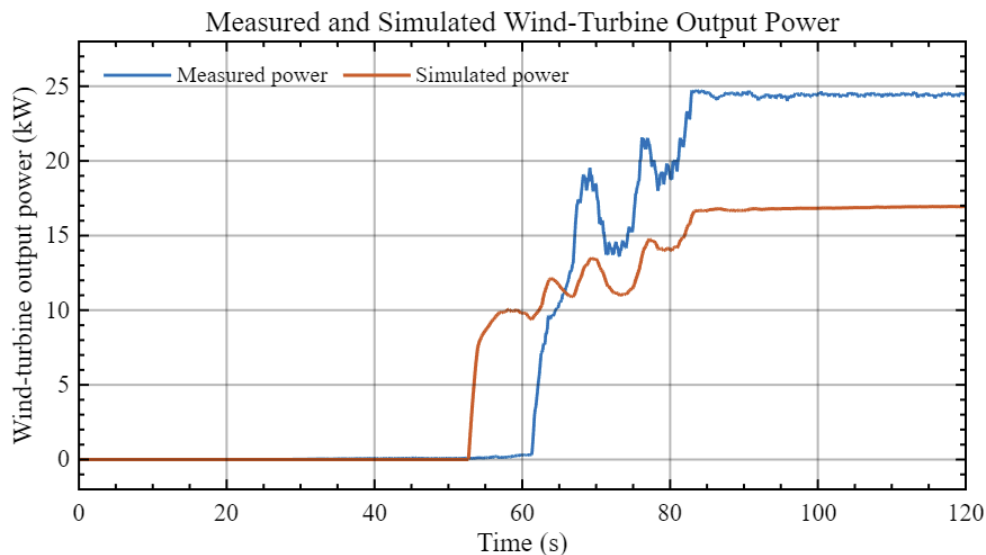


**Figure 4.19:** Reference and simulated wind-turbine output power.

The measured/reference and simulated power signals are shown for different interpretive purposes. The measured/reference signal provides the normal-operation power trajectory associated with the inherited wind-turbine data, whereas the sim-

ulated signal represents the model output when the EMS curtailment request is applied through the wind-spill path. The comparison is therefore not used as an error calculation between two identical operating cases.

During the initial portion of the interval, the timing difference between the two trajectories is associated with the start-up representation of the wind-turbine model. During the later operating period, after approximately 84 s, the measured/reference output is close to 24.5 kW, whereas the simulated output settles at approximately 16.5–17 kW. This reduction is interpreted together with the simultaneously active curtailment and wind-spill command presented below.

#### 4.6.4 Battery Dispatch and SOC Evolution

Figures 4.20 and 4.21 show the battery-power reference generated by the EMS and the corresponding constrained battery response.

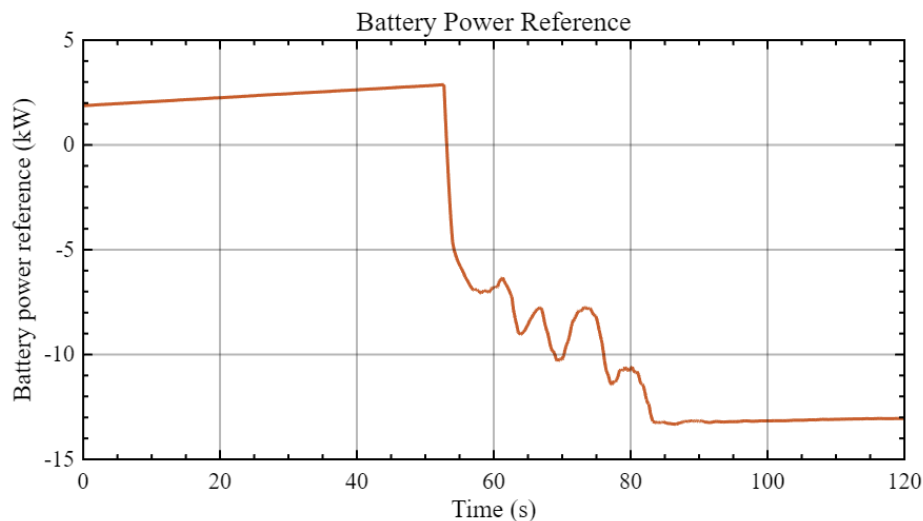
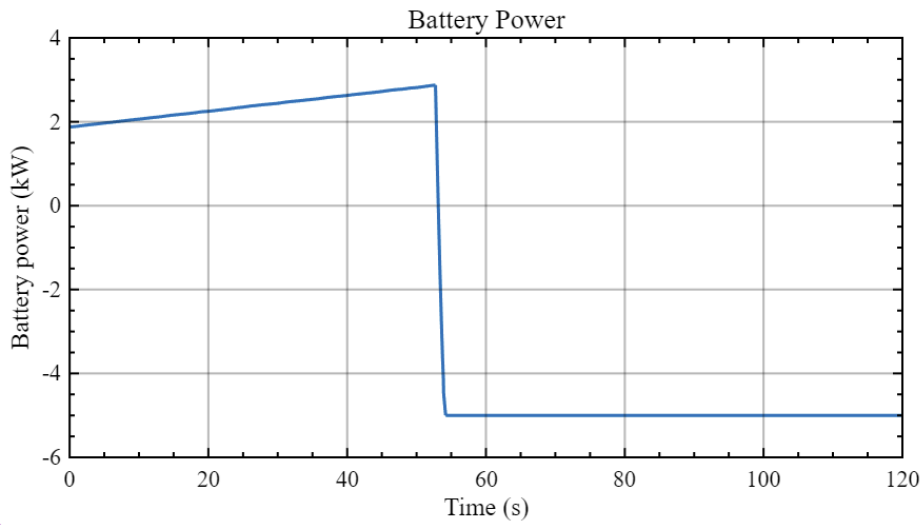


**Figure 4.20:** Battery-power reference  $P_{\text{batt,ref}}$  generated by the EMS during the 0–120 s short-term simulation. Positive power represents a discharge request and negative power represents a charging request.

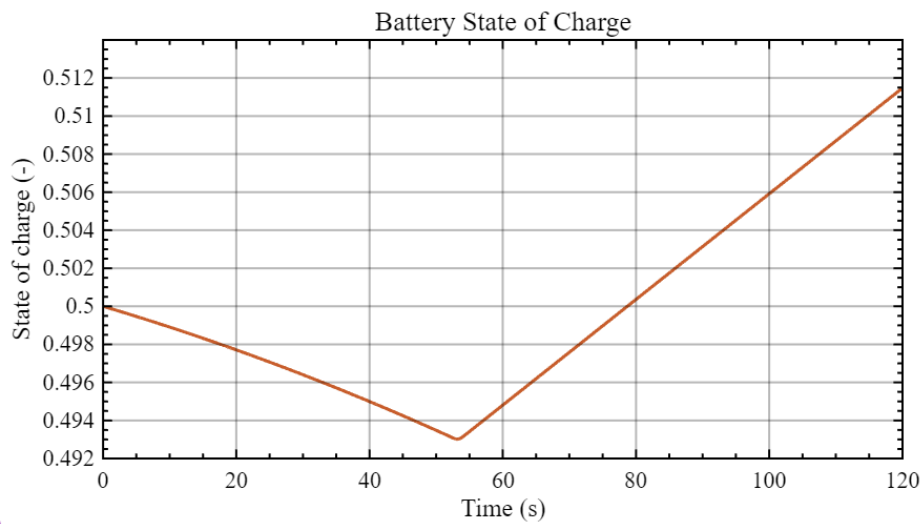
During the initial start-up portion of the simulation, the battery-power reference is positive and increases from approximately 2 kW to approximately 3 kW. The constrained battery response follows this discharge request. When the wind-turbine output becomes available at approximately 53 s, the battery-power reference changes sign and the EMS requests charging. As wind-power production continues to increase, the requested charging power reaches approximately  $-13$  kW, while the constrained battery power is limited to approximately  $-5$  kW. Consequently, the battery absorbs part of the renewable surplus, while the remaining portion must be handled by the subsequent curtailment action.

Figure 4.22 shows the associated SOC evolution.

The SOC decreases from approximately 0.500 to approximately 0.493 during the initial battery-discharge interval. After the transition to battery charging at approximately 53 s, the SOC increases continuously and reaches approximately 0.511 at the end of the simulation. This response is consistent with the sign convention



**Figure 4.21:** Constrained battery power  $P_{\text{batt}}$  during the 0–120 s short-term simulation. Positive power represents discharge and negative power represents charging.



**Figure 4.22:** Battery SOC in the short-term simulation.

and magnitude of the constrained battery power: positive battery power supplies the initial deficit, whereas sustained negative battery power stores a portion of the subsequent renewable surplus.

#### 4.6.5 Mismatch Identification and Battery-Limited Residual Power

Figures 4.23 and 4.24 show the original deficit and surplus calculated before constrained battery action.

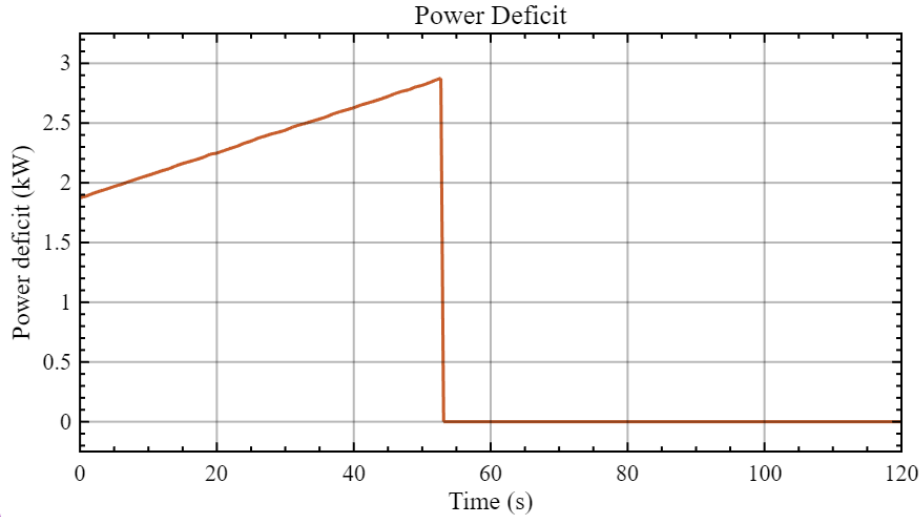


**Figure 4.23:** Original power deficit  $P_{\text{deficit}}$  before constrained battery action during the 0–120 s short-term simulation.

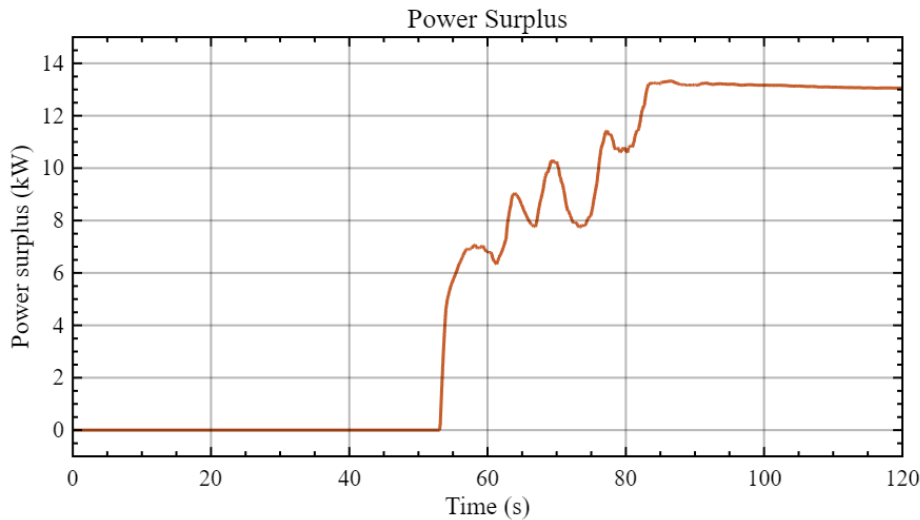


**Figure 4.24:** Original power surplus  $P_{\text{surplus}}$  before constrained battery action during the 0–120 s short-term simulation.

Before the wind-turbine output is established, the EMS identifies a deficit of approximately 2–3 kW. This deficit is removed by the battery-discharge action. At approximately 53 s, the original deficit becomes zero and a renewable surplus appears.

The surplus rises with the increasing wind-turbine output and reaches approximately 13 kW during the comparatively steady operating period.

Figures 4.25 and 4.26 show the residual mismatch after constrained battery action.

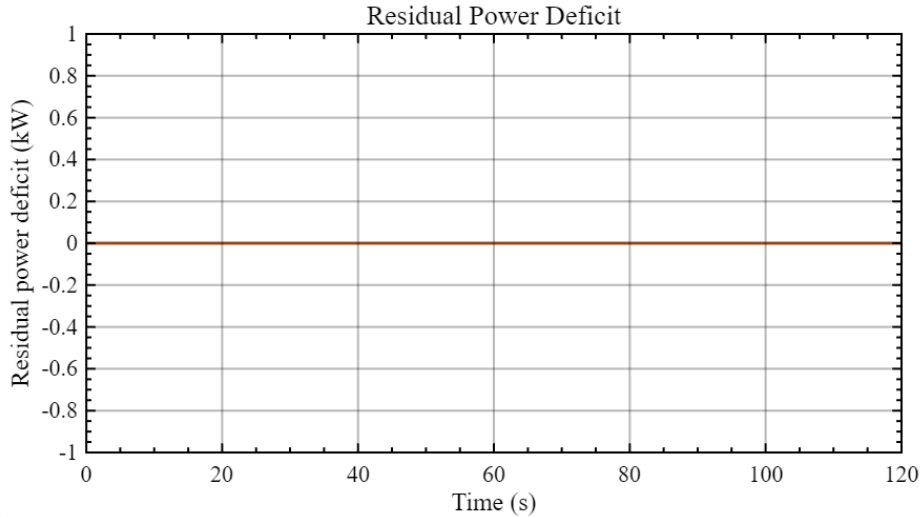


**Figure 4.25:** Residual power deficit  $P_{\text{deficit,res}}$  after constrained battery action during the 0–120 s short-term simulation.

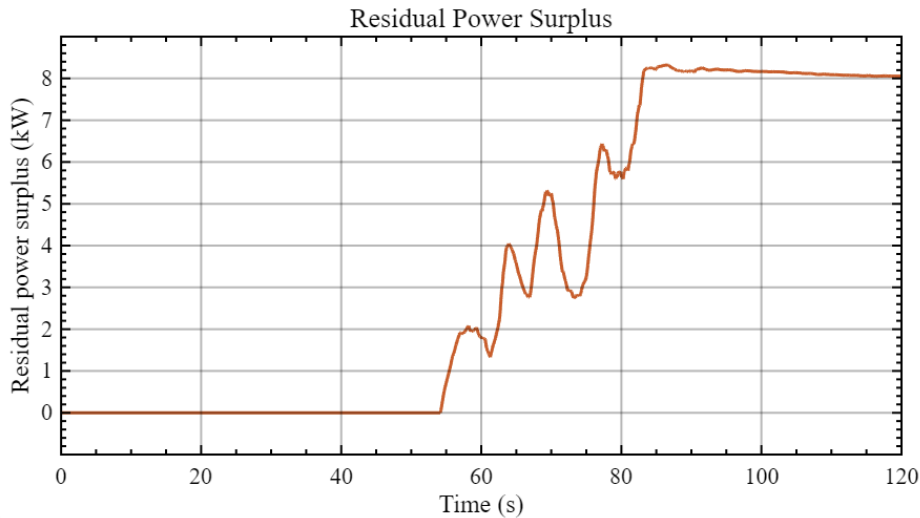


**Figure 4.26:** Residual power surplus  $P_{\text{surplus,res}}$  after constrained battery action during the 0–120 s short-term simulation.

The residual deficit remains zero throughout the presented case. During the initial deficit condition, this indicates that the battery-discharge action is sufficient to cover the required balancing power. After the system enters the surplus condition, the residual surplus becomes positive because the battery charging response is constrained to approximately  $-5$  kW. In the later steady portion of the simulation, the original surplus is approximately 13 kW, while the residual surplus is approximately 8 kW. This is consistent with the battery absorbing approximately 5 kW of the surplus and leaving the remainder for wind-power curtailment.

### 4.6.6 Curtailment, Load Shedding, and Wind-Spill Transfer

Figure 4.27 shows the curtailment request generated by the EMS. Owing to the direct interface assignment defined in Equation (4.1), the plotted quantity is also the wind-spill command supplied to the turbine-control path.

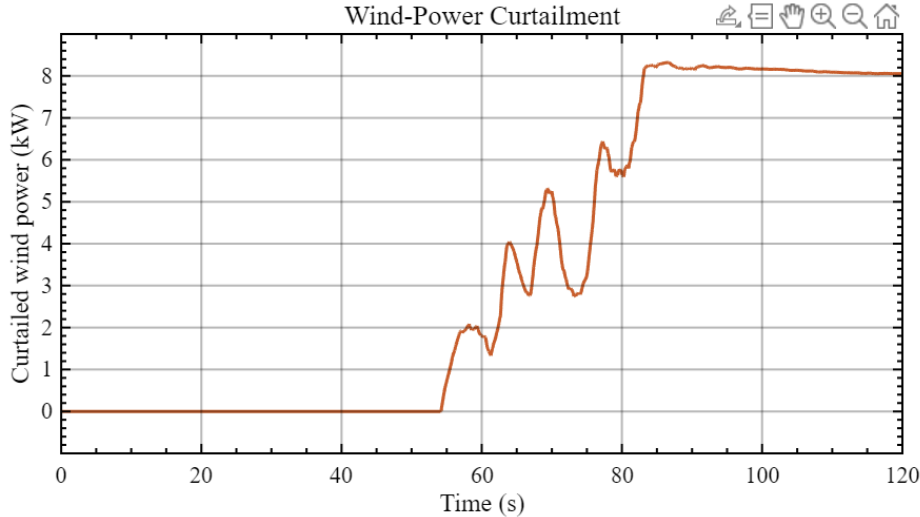


**Figure 4.27:** EMS wind-power curtailment request  $P_{\text{curt}}$ , supplied directly as the wind-spill command  $P_{\text{spill}}$  during the 0–120 s short-term simulation.

The curtailment request remains zero while no residual surplus exists. It becomes positive after the transition to the surplus condition and follows the residual-surplus trajectory. After approximately 84 s,  $P_{\text{curt}} = P_{\text{spill}}$  settles at approximately 8 kW, consistent with the residual surplus remaining after the battery charging constraint is applied.

Since  $P_{\text{spill}}$  is directly supplied by  $P_{\text{curt}}$ , a separate second plot of the identical trajectory is not required for the result interpretation. The turbine-side consequence of this command is evaluated from the simulated blade-pitch and realised wind-power response.

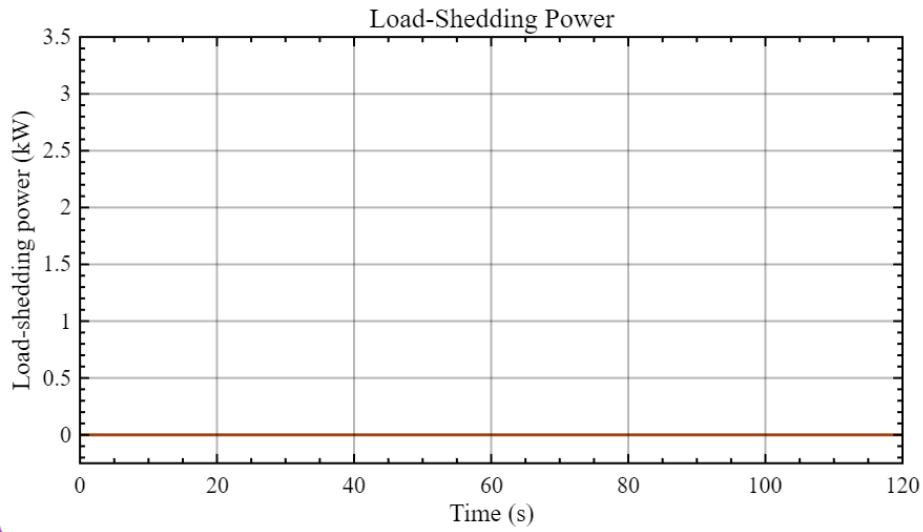
Figure 4.28 shows the load-shedding request.

The load-shedding request remains zero throughout the simulation. This result is consistent with  $P_{\text{deficit, res}} = 0$ : the initial deficit is covered by battery discharge, and the subsequent operating condition is dominated by surplus rather than unserved demand. The additional EMS-level validation case in Section 4.5 complements this short-term result by showing the response when a residual deficit is intentionally created.

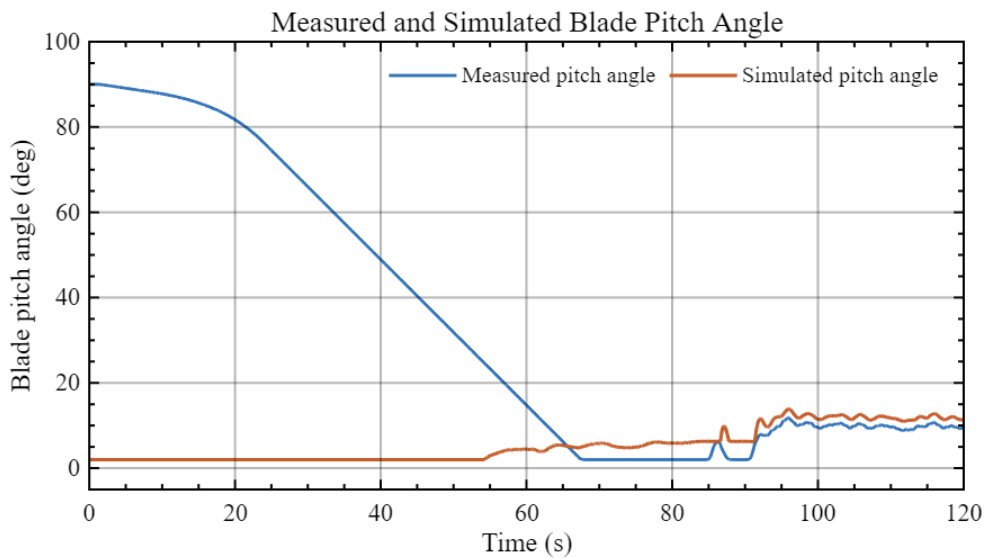
### 4.6.7 Blade-Pitch Response and Realised Wind-Power Reduction

Figure 4.29 compares the measured/reference blade-pitch angle with the simulated blade-pitch response.

During the initial start-up period, the measured/reference blade-pitch angle decreases from approximately  $90^\circ$ , whereas the simulated blade-pitch angle remains



**Figure 4.28:** Load-shedding request  $P_{\text{loadshed}}$  during the 0–120 s short-term simulation.



**Figure 4.29:** Reference and simulated blade-pitch signals.

close to the minimum operating pitch of approximately  $2^\circ$ . These two curves are not interpreted as coincident trajectories during turbine start-up: the measured/reference trajectory contains the normal-operation start-up behaviour in the inherited data, whereas the simulated trajectory represents the initialised model response.

The presence of a simulated blade-pitch angle near  $2^\circ$  during the initial interval does not imply immediate electrical power production. The realised wind-turbine output also depends on the establishment of the turbine-side dynamic state and generator-control response. Therefore, the initial zero  $P_{\text{wind}}$  is interpreted as a start-up response of the dynamic wind-turbine model.

After the residual surplus and wind-spill command become active, the simulated blade-pitch angle moves away from its minimum setting and reaches approximately  $10\text{--}12^\circ$  in the later operating period. This response is consistent with pitch-based wind-power curtailment: a higher pitch setting reduces the aerodynamic power capture represented by the wind-turbine model.

The relationship between wind availability, wind-spill command, and realised wind-power output is particularly clear after approximately 84 s. During this period,

$$P_{\text{wind,avail}} \approx 25 \text{ kW}, \quad P_{\text{spill}} \approx 8 \text{ kW}, \quad P_{\text{wind}} \approx 16.5\text{--}17 \text{ kW}. \quad (4.2)$$

Accordingly, the simulated response approximately satisfies

$$P_{\text{wind}} + P_{\text{spill}} \approx P_{\text{wind,avail}}, \quad (4.3)$$

which supports the interpretation that the residual surplus requested by the EMS is transferred into the wind-spill path and represented as reduced realised wind-turbine output.

## 4.7 Key Result Values

Table 4.3 summarises the main numerical values observed from the presented result figures. The table is included to make the graphical results easier to interpret and to connect the long-term, additional deficit, and short-term cases.

The key values show that the EMS behaves consistently across the three result groups. It charges the battery and curtails wind power under residual surplus, discharges the battery and sheds load under residual deficit, and transfers the short-term curtailment request into the inherited wind-spill path.

## 4.8 Integrated Interpretation

The long-term, additional deficit, and short-term results jointly demonstrate the supervisory power-balancing sequence of the developed model. In the long-term EMS/BESS simulation, prescribed operating profiles are processed by the EMS and BESS interface to generate a battery-power request, constrained battery action, SOC evolution, residual mismatch, wind-power curtailment request, and load-shedding request. The long-term case thereby demonstrates the supervisory hierarchy over an extended surplus-dominated operating period.

**Table 4.3:** Key numerical results from the presented simulations.

Quantity	Symbol	Approx. value	Case
Battery charging response	$P_{\text{batt}}$	−5 kW	Long-term surplus case
Initial deficit peak	$P_{\text{deficit}}$	13–14 kW	Deficit-validation case
Battery discharge response	$P_{\text{batt}}$	+5 kW	Deficit-validation case
Local SOC response	SOC	Local decrease around 800–860 s	Deficit-validation case
Residual deficit peak	$P_{\text{deficit,res}}$	8–9 kW	Deficit-validation case
Load-shedding request peak	$P_{\text{loadshed}}$	8–9 kW	Deficit-validation case
Available wind power	$P_{\text{wind,avail}}$	25 kW	Short-term later period
Wind-spill request	$P_{\text{spill}}$	8 kW	Short-term later period
Realised wind power	$P_{\text{wind}}$	16.5–17 kW	Short-term later period
Blade-pitch response	$\beta_{\text{sim}}$	10–12°	Short-term later period

The additional deficit validation case adds the opposite corrective branch to the discussion. When the prescribed load demand is higher than the renewable contribution and the available battery discharge response, the EMS uses the battery first; this can be seen from the local SOC decrease during the main deficit interval. After that, the EMS calculates the residual deficit that is still left, and this remaining part is then sent to load shedding. This shows that the load-shedding branch is not only included in the model structure, but can also be activated when the operating condition requires it.

In the 0–120 s short-term interaction case, the complete initial interval is kept, so that the turbine start-up and the dynamic-state establishment are still visible in the analysis. The wind-turbine output is zero at the beginning, and then it increases into a power-producing condition. During the initial deficit condition, the battery supplies the needed balancing power, so the residual deficit remains zero. After wind-power production is established, the EMS detects surplus power and requests battery charging. Since the battery charging response is limited, a residual surplus still remains, and this part is then converted into the wind-power curtailment command.

Through the direct connection  $P_{\text{spill}} = P_{\text{curt}}$ , the residual-surplus correction is supplied to the wind-turbine control path. The resulting simulated blade-pitch increase and the reduction of realised wind-turbine output relative to the available wind-power estimate provide the turbine-side response associated with the EMS request. In the later operating period, the approximate consistency among available wind power, curtailed power, and realised output power further supports this interpretation.

The measured/reference wind-turbine signals and the simulated EMS-controlled signals are interpreted separately on purpose. The measured/reference signals give an operating reference for normal turbine operation, while the simulated signals show the dynamic model response when the supervisory wind-spill interaction is applied. Therefore, the difference between these signals is used to explain the effect of the turbine-side command; it is not used as a direct simulation error between two identical cases.

## 4.9 Summary of Result Findings

The main result findings are summarised as follows.

First, the long-term EMS/BESS simulation demonstrates a consistent supervisory sequence under the analysed source and load conditions. Battery charging is requested during renewable surplus, SOC increases accordingly, residual surplus is identified when the constrained BESS response is insufficient, and the remaining surplus is assigned to wind-power curtailment.

Second, the additional deficit validation case verifies the load-shedding branch of the EMS. When the prescribed load demand creates a deficit larger than the battery can cover, the constrained battery discharge reaches approximately 5 kW and the SOC shows a local decrease during the same interval. The remaining residual deficit reaches approximately 8–9 kW, and the load-shedding request follows this residual deficit. This confirms the implemented sequence from deficit identification to battery

support, battery state response, and then to load shedding.

Third, the complete 0–120 s short-term interval preserves the wind-turbine start-up response and avoids interpreting an intermediate-time model initialisation as a physical zero-power event. The simulated wind-turbine output becomes non-zero after the initial start-up interval and enters a comparatively stable power-producing condition during the later part of the simulation.

Fourth, the short-term battery response demonstrates the transition from deficit handling to surplus handling. The battery initially discharges to eliminate the power deficit and subsequently charges when wind-power production becomes available. Its constrained charging response leaves a residual surplus of approximately 8 kW in the later operating period.

Fifth, the residual-surplus signal is transferred to the turbine side through the implemented assignment  $P_{\text{spill}} = P_{\text{curt}}$ . The associated simulated blade-pitch response and the limited realised wind-turbine power are consistent with the intended wind-spill mechanism.

The simulated blade-pitch response and the reduction in realised wind-turbine output are consistent with the wind-spill mechanism reported for the inherited Chalmers turbine model, in which output reduction is realised through controller adjustments including blade-pitch action [17].

Finally, the combined results demonstrate an islanded-operation supervisory framework in which prescribed photovoltaic and load conditions, dynamically represented wind-turbine production, battery dispatch, SOC evolution, residual mismatch, wind-power curtailment, load-shedding activation, and turbine-side pitch response are analysed within one coherent power-balancing sequence.

# 5

## Conclusion

This thesis developed and evaluated a supervisory simulation framework for the islanded operation of a hybrid renewable power system, which consists of a wind turbine, photovoltaic generation, battery energy storage, and local load demand. The study combines an inherited Chalmers wind-turbine model with a newly implemented energy-management layer and a simplified BESS interface, so that wind-turbine behaviour can be studied as part of a coordinated islanded power-balance problem.

The main contribution of this thesis is to design and implement an energy management system (EMS) based on power balance. The EMS calculates the mismatch between renewable energy and load according to the actual wind turbine output power, photovoltaic power and load demand. Based on this mismatch, the EMS generates a battery-power reference, applies battery power and state-of-charge constraints, determines the remaining deficit or surplus after battery action, and activates wind curtailment or load shedding when the battery cannot remove the imbalance by itself. This structure meets the core requirements of islanded operation: local generation, storage, and consumption must be coordinated without relying on continuous support from a strong external grid.

A key modelling distinction established in the thesis is the difference between available wind power and realised wind-turbine output. The available wind-power signal  $P_{\text{wind,avail}}$  represents the estimated wind-side availability produced by the inherited wind model and is retained as a reference for interpreting turbine operation. The realised wind-turbine output  $P_{\text{wind}}$ , however, is the simulated power delivered after the inherited wind-turbine dynamics and, when activated, the wind-spill and blade-pitch response. In accordance with the verified Simulink routing,  $P_{\text{wind}}$  is used in the supervisory renewable aggregation and as the wind-side input of the implemented Wind Curtailment subsystem.

Another important contribution is the treatment of wind curtailment as a turbine-side control interaction. Instead of reducing wind power by direct algebraic subtraction, the EMS curtailment request  $P_{\text{curt}}$  is connected to the inherited wind-spill input as  $P_{\text{spill}}$ . The wind-turbine model then responds through its wind-spill and blade-pitch mechanism. The short-term results show that, when a renewable surplus remains after battery charging is constrained, the curtailment request becomes active, the simulated blade-pitch angle increases, and the realised wind-turbine output is reduced relative to the available wind-power reference. This behaviour is consistent with the intended wind-spill-based curtailment mechanism.

The short-term integrated simulation demonstrates the transition between deficit-handling and surplus-handling operation. During the initial interval, the battery

supplies the detected deficit and the residual deficit remains zero. After wind-power production is established, the battery reference changes from discharging to charging. When the charging response reaches its implemented limit, residual surplus remains and is transferred to the wind-spill path through  $P_{\text{spill}} = P_{\text{curt}}$ . The associated blade-pitch response and realised wind-power reduction show that the inherited wind model and the developed EMS are coupled in a physically interpretable way. The long-term EMS/BESS simulation complements the short-term case by showing how the developed supervisory structure behaves over a longer operating interval. Driven by time-varying wind, photovoltaic, and load profiles, the EMS generates battery-reference power, constrained battery power, SOC evolution, original mismatch, residual mismatch, and corrective-action requests. In the presented long-term surplus-dominated condition, the battery charges until its permissible response is limited, after which remaining residual surplus is assigned to wind-power curtailment.

To check the other corrective branch, an additional EMS-level case with a deficit-dominated condition was added by using a prescribed high-load interval. In this case, the initial power deficit is larger than the battery discharge capability; the battery first supplies about 5 kW, and after that a residual deficit still remains, so this remaining part is changed into a load-shedding request. This extra case shows that the EMS has a working deficit-handling branch, and that load shedding is only used for the part of the demand that cannot be covered after the possible battery discharge.

The simplified system-level interface in this thesis is used to organise the corrected power variables for the supervisory power-balance interpretation. In this interface, the realised wind-turbine output is passed forward after the wind-spill response, so the curtailment is not subtracted again. The effective load also includes the effect of the load-shedding request. By using this interpretation, the EMS commands and the power quantities discussed in the simulation results can stay consistent.

Overall, the thesis shows that the islanded operation of a hybrid wind-solar-battery system can be arranged by using a clear supervisory control structure. The developed model coordinates battery dispatch, wind-spill-based curtailment, and load shedding in a defined priority order; it also shows how the inherited wind-turbine model can be connected with the new EMS without removing the original turbine-side dynamics. Therefore, the final model gives a reasonable basis for analysing local active-power balancing in an islanded renewable power system.

Future work can continue from this model by adding more detail to the component and converter models. For example, a more detailed photovoltaic model could include irradiance changes, DC-link behaviour, and converter control. The battery model could also be improved by adding voltage dynamics, efficiency changes, thermal effects, and ageing-related limits. In future work, a downstream electrical model could include a detailed grid-forming converter and a three-phase network model, so that voltage, frequency, current, and active-power behaviour can be studied when renewable power and load demand change quickly. In addition, more parameter studies on battery capacity, charge and discharge limits, wind conditions, PV profiles, and load categories could give more information about the sizing and robustness of islanded hybrid power systems.

# Bibliography

- [1] M. Jafari, A. Botterud, and A. Sakti, “Decarbonizing power systems: A critical review of the role of energy storage,” *Renewable and Sustainable Energy Reviews*, vol. 158, art. no. 112077, 2022, doi: 10.1016/j.rser.2022.112077.
- [2] R. H. Lasseter and P. Piagi, “Microgrid: A conceptual solution,” in *2004 IEEE 35th Annual Power Electronics Specialists Conference*, 2004, vol. 6, pp. 4285–4290, doi: 10.1109/PESC.2004.1354758.
- [3] D. E. Olivares, A. Mehrizi-Sani, A. H. Etemadi, C. A. Cañizares, R. Iravani, M. Kazerani, A. H. Hajimiragha, O. Gomis-Bellmunt, M. Saeedifard, R. Palma-Behnke, G. A. Jiménez-Estévez, and N. D. Hatziargyriou, “Trends in Microgrid Control,” *IEEE Transactions on Smart Grid*, vol. 5, no. 4, pp. 1905–1919, Jul. 2014, doi: 10.1109/TSG.2013.2295514.
- [4] Q. Hassan, S. Algburi, A. Z. Sameen, H. M. Salman, and M. Jaszczur, “A review of hybrid renewable energy systems: Solar and wind-powered solutions: Challenges, opportunities, and policy implications,” *Results in Engineering*, vol. 20, art. no. 101621, 2023, doi: 10.1016/j.rineng.2023.101621.
- [5] F. Weschenfelder, G. N. P. Leite, A. C. A. da Costa, F. V. da Silva, C. F. Detzel, and L. A. Isorna, “A review on the complementarity between grid-connected solar and wind power systems,” *Journal of Cleaner Production*, vol. 257, art. no. 120617, 2020, doi: 10.1016/j.jclepro.2020.120617.
- [6] O. Carlson, *Island operation with wind turbines and batteries*, project brief for master’s thesis work, Chalmers University of Technology, 2026.
- [7] E. Planas, A. Gil-de-Muro, J. Andreu, I. Kortabarria, and I. Martínez de Alegría, “General aspects, hierarchical controls and droop methods in microgrids: A review,” *Renewable and Sustainable Energy Reviews*, vol. 17, pp. 147–159, 2013, doi: 10.1016/j.rser.2012.09.032.
- [8] O. Palizban and K. Kauhaniemi, “Hierarchical control structure in microgrids with distributed generation: Island and grid-connected mode,” *Renewable and Sustainable Energy Reviews*, vol. 44, pp. 797–813, 2015, doi: 10.1016/j.rser.2015.01.008.
- [9] U. B. Tayab, M. A. Roslan, L. J. Hwai, and M. Kashif, “A review of droop control techniques for microgrid,” *Renewable and Sustainable Energy Reviews*, vol. 76, pp. 717–727, 2017, doi: 10.1016/j.rser.2017.03.028.
- [10] K. De Brabandere, B. Bolsens, J. Van den Keybus, A. Woyte, J. Driesen, and R. Belmans, “A voltage and frequency droop control method for parallel inverters,” *IEEE Transactions on Power Electronics*, vol. 22, no. 4, pp. 1107–1115, Jul. 2007, doi: 10.1109/TPEL.2007.900456.

- [11] P. Satish Kumar, R. P. S. Chandrasena, V. Ramu, G. N. Sreenivas, and K. Victor Sam Moses Babu, “Energy Management System for Small Scale Hybrid Wind Solar Battery Based Microgrid,” *IEEE Access*, vol. 8, pp. 8336–8345, 2020, doi: 10.1109/ACCESS.2020.2964052.
- [12] M. Elkazaz, M. Sumner, and D. Thomas, “Energy management system for hybrid PV-wind-battery microgrid using convex programming, model predictive and rolling horizon predictive control with experimental validation,” *International Journal of Electrical Power & Energy Systems*, vol. 115, art. no. 105483, 2020, doi: 10.1016/j.ijepes.2019.105483.
- [13] M. F. Zia, M. Nasir, E. Elbouchikhi, M. Benbouzid, J. C. Vasquez, and J. M. Guerrero, “Energy management system for a hybrid PV-Wind-Tidal-Battery-based islanded DC microgrid: Modeling and experimental validation,” *Renewable and Sustainable Energy Reviews*, vol. 159, art. no. 112093, 2022, doi: 10.1016/j.rser.2022.112093.
- [14] W. Ely, M. L. Doumbia, T. Tahar, S. P. Betoka, and H. Hamza, “Energy Management of an Autonomous Hybrid Wind-Photovoltaic Microgrid with Battery Storage,” in *2023 12th International Conference on Renewable Energy Research and Applications (ICRERA)*, 2023, pp. 492–498, doi: 10.1109/ICRERA59003.2023.10269369.
- [15] Y. Zhang, H. J. Jia, and L. Guo, “Energy management strategy of islanded microgrid based on power flow control,” in *2012 IEEE PES Innovative Smart Grid Technologies (ISGT)*, 2012, pp. 1–8, doi: 10.1109/ISGT.2012.6175644.
- [16] A. Bonfiglio, M. Brignone, M. Invernizzi, A. Labella, D. Mestriner, and R. Procopio, “A Simplified Microgrid Model for the Validation of Islanded Control Logics,” *Energies*, vol. 10, no. 8, art. no. 1141, 2017, doi: 10.3390/en10081141.
- [17] M. Eriksson, *Frekvensstyrning med vindkraft*, Technical Report 2023:3, Department of Electrical Engineering, Division of Electric Power Engineering, Chalmers University of Technology, Gothenburg, Sweden, 2023.
- [18] A. Mal and S. A. Bukhari, *Islanded Operation of Wind Turbine with Solar Power and Battery Storage: A Step Towards Fossil Free Energy*, Master’s Thesis, Department of Electrical Engineering, Chalmers University of Technology, Gothenburg, Sweden, 2024.
- [19] J. Aho, A. Buckspan, J. Laks *et al.*, “A tutorial of wind turbine control for supporting grid frequency through active power control,” in *2012 American Control Conference*, 2012, pp. 3120–3131.
- [20] Y. Qi, H. Deng, X. Liu, and Y. Tang, “Synthetic inertia control of grid-connected inverter considering the synchronization dynamics,” *IEEE Transactions on Power Electronics*, vol. 37, no. 2, pp. 1411–1421, 2022.
- [21] E. Planas, J. Andreu, J. I. Gárate, I. Martínez de Alegría, and E. Ibarra, “AC and DC technology in microgrids: A review,” *Renewable and Sustainable Energy Reviews*, vol. 43, pp. 726–749, 2015, doi: 10.1016/j.rser.2014.11.067.
- [22] J. Alshehri, M. Khalid, and A. Alzahrani, “An Intelligent Battery Energy Storage-Based Controller for Power Quality Improvement in Microgrids,” *Energies*, vol. 12, no. 11, art. no. 2112, 2019, doi: 10.3390/en12112112.
- [23] D. Arcos-Avilés, J. Pascual, L. Marroyo, P. Sanchis, and F. Guinjoan, “Fuzzy Logic-Based Energy Management System Design for Residential Grid-

Connected Microgrids,” *IEEE Transactions on Smart Grid*, vol. 9, no. 2, pp. 530–543, Mar. 2018, doi: 10.1109/TSG.2016.2555245.



# A

## Supplementary Material

### A.1 Key Supervisory Variables

For clarity, the main supervisory variables used throughout the thesis are summarised below:

- $P_{\text{wind,avail}}$ : rated-power-capped available wind-power estimate generated by the inherited wind-turbine model and retained as a wind-side availability reference;
- $P_{\text{wind}}$ : realised simulated wind-turbine output after the inherited turbine dynamics and, when activated, the wind-spill and blade-pitch response; this is the wind-power signal used in the EMS and the implemented Wind Curtailment subsystem;
- $P_{\text{pv}}$ : equivalent AC-side photovoltaic active-power contribution supplied to the EMS power-balance interface; the detailed DC-side PV-panel behaviour and inverter conversion dynamics are not separately represented in the implemented model;
- $P_{\text{load}}$ : original load demand before load-shedding correction;
- $P_{\text{batt,ref}}$ : battery-reference power calculated by the EMS before battery-power and SOC limitations;
- $P_{\text{batt}}$ : final constrained battery power after charging/discharging and SOC constraints; positive values denote discharge and negative values denote charging;
- $P_{\text{deficit}}$  and  $P_{\text{surplus}}$ : original deficit and surplus components before feasible battery action;
- $P_{\text{deficit,res}}$  and  $P_{\text{surplus,res}}$ : residual mismatch components after feasible battery action;
- $P_{\text{curt}}$ : EMS wind-curtailment request generated from residual surplus; in the implemented Wind Curtailment subsystem,  $P_{\text{curt}} = \min(P_{\text{surplus,res}}, P_{\text{wind}})$ ;
- $P_{\text{spill}}$ : spilling-power command passed to the inherited wind-spill path; in the implemented connection,  $P_{\text{spill}} = P_{\text{curt}}$ ;
- $P_{\text{loadshed}}$ : load-shedding request generated from residual deficit;
- $P_{\text{load,eff}}$ : effective load after load-shedding correction;
- $P_{\text{pv,eff}}$ : effective photovoltaic contribution used in downstream supervisory power-balance interpretation; in this thesis,  $P_{\text{pv,eff}} = P_{\text{pv}}$ ;
- $P_{\text{batt,eff}}$ : effective battery power used in downstream supervisory power-balance interpretation; in this thesis,  $P_{\text{batt,eff}} = P_{\text{batt}}$ ;
- $P_{\text{net}}$ : net active-power quantity used for downstream supervisory power-balance interpretation;

- *SOC*: state of charge of the battery generated by the simplified BESS interface in response to the constrained battery-power trajectory.

## A.2 Validation Structure Used in the Thesis

The final validation structure used in the thesis is organised into three complementary parts:

1. **Long-term EMS/BESS case.** This case uses prescribed time-varying wind, photovoltaic, and load profiles over an 1800 s horizon to evaluate battery-reference generation, constrained battery charging, SOC evolution, residual surplus, and the wind-curtailment request under a mainly surplus-dominated operating condition. The SOC trajectory is interpreted as a simulated BESS output, rather than as an externally prescribed input profile.
2. **Additional deficit and load-shedding validation case.** This EMS-level case applies a prescribed high-load interval in order to verify the deficit-side control branch. The imposed shortage first produces a battery-discharge response subject to the implemented power and SOC constraints. When the allowable battery response is insufficient to remove the full mismatch, the remaining residual deficit is converted into a load-shedding request.
3. **Short-term integrated EMS–wind-turbine case.** This case uses the inherited wind-turbine subsystem together with the EMS to evaluate the transition from deficit to surplus, the battery sign change, residual surplus formation, and the wind-spill-based curtailment response. In this case, the EMS curtailment request is passed to the inherited wind-spill input through  $P_{\text{spill}} = P_{\text{curt}}$ . The resulting blade-pitch response and realised wind-turbine output are then used to interpret the turbine-side effect of the curtailment command.

Together, these three cases verify the supervisory sequence developed in the thesis. The battery is applied first within its implemented constraints; residual surplus is assigned to wind curtailment; residual deficit is assigned to load shedding; and the short-term wind-spill request is realised through the inherited turbine-side response.

## A.3 Role of the Present Appendix

This appendix provides a compact reference for the main supervisory variables and for the validation structure used in the thesis. It is intended to support the readability of the main chapters and to consolidate the signal definitions used in the theory, implementation, and result discussions, without introducing additional validation claims beyond those evaluated in the main text.

DEPARTMENT OF ELECTRICAL ENGINEERING  
CHALMERS UNIVERSITY OF TECHNOLOGY  
Gothenburg, Sweden  
[www.chalmers.se](http://www.chalmers.se)



**CHALMERS**  
UNIVERSITY OF TECHNOLOGY